Farkas *et al. Geothermal Energy* (2025) 13:20
https://doi.org/10.1186/s40517-025-00344-7

Geothermal Energy

RESEARCH Open Access

Comparison of stimulation techniques in a geothermal injection well in a sedimentary aquifer in Szentes, Hungary

Márton Pál Farkas[1,2*], Gábor Magyar[3], Hannes Hofmann[1,4], Günter Zimmermann[1,4] and Ferenc Fedor[2]

*Correspondence:
farkas@gfz.de

[1] Section 4.3 Geoenergy, GFZ Helmholtz Centre for Geosciences, Telegrafenberg, 14473 Potsdam, Germany
[2] Department of Geology and Meteorology, Institute of Geography and Earth Sciences, University of Pécs, Ifjúság Útja 6, 7624 Pécs, Hungary
[3] CROST Regional Development Nonprofit Ltd., Rákóczi Út 13/B 1/8, 7621 Pécs, Hungary
[4] Institute of Applied Geosciences, Technical University Berlin, Ernst-Reuter-Platz 1, 10587 Berlin, Germany

Abstract

The Upper Pannonian (UP) sandstone formation in Hungary has been utilized for thermal water production without reinjection since the 1960s. However, there is an increasing need for setting up geothermal doublets or triplets, where used water is expected to be reinjected into the same formation. Sustainable injection into porous sandstone rock formation is not straightforward. Thus, the Hungarian research and development project "Development of a well completion technology for sustainable and cost-effective reinjection of thermal water" aims at designing a methodology for sustaining the injectivity of geothermal wells in UP sandstone reservoirs. In this case study, we present an intervention approach of an old geothermal production well for reinjection at the Szentes Geothermal Field. Based on the evaluation of well conditions, the injectivity decline may be associated with reservoir characteristics, i.e., low transmissibility, mineral precipitation or local particle migration. Thus, a stimulation program was designed, where various techniques such as hydraulic fracturing, acid treatment and skin frac experiment were conducted. The novelty of this study is that to the best of our knowledge, the skin frac technique has been applied for the first time in a geothermal injection well worldwide. Based on the comparison of the various stimulation experiments, the injectivity reduction is related to phenomena in the near-wellbore area, i.e., mechanical clogging due to fines migration in the reservoir. The largest injectivity enhancement was observed due to skin frac experiment and pump lift, which was not part of the original stimulation program. The skin frac method has the potential for providing injectivity enhancement of recompleted wells in poorly cemented sandstone formations, but further field demonstration with optimized design is required. The results of this well treatment, such as regular conduction of pump lift and recommendations for proper design of skin frac treatment can be used in designing long-term reinjection tests in loose sandstone formations in geothermal reservoirs. Furthermore, future study should focus on the investigation of the link between pressure depletion due to overexploitation, subsequent compaction and land subsidence as well as injectivity problems.

Keywords: Upper Pannonian sandstone, Injectivity decline, Clogging, Fines migration, Stimulation techniques, Skin frac

© The Author(s) 2025. **Open Access** This article is licensed under a Creative Commons Attribution 4.0 International License, which permits use, sharing, adaptation, distribution and reproduction in any medium or format, as long as you give appropriate credit to the original author(s) and the source, provide a link to the Creative Commons licence, and indicate if changes were made. The images or other third party material in this article are included in the article's Creative Commons licence, unless indicated otherwise in a credit line to the material. If material is not included in the article's Creative Commons licence and your intended use is not permitted by statutory regulation or exceeds the permitted use, you will need to obtain permission directly from the copyright holder. To view a copy of this licence, visit http://creativecommons.org/licenses/by/4.0/.

Introduction

In Hungary, geothermal energy has been utilized since the nineteenth century in the Pannonian Basin. The geothermal exploitation is concentrated in the South-Eastern part of the country due to elevated geothermal gradient of ~ 45–50 °C/km compared to other parts of the country, which can be linked to a relatively thin crust and lithosphere (Horváth et al. 2015; Lenkey et al. 2021). In that area thermal water from Upper Pannonian (UP) sandstone formations, especially the Újfalu Formation, has been produced since the 1960s (Szanyi and Kovács 2010). Thermal water produced mainly from the loose and poorly consolidated UP sandstone formation with relatively high permeability is utilized for district heating, balneological as well as agricultural purposes with a total installed capacity of approx. 1014 $MW_{thermal}$ (EGEC Market Report 2023). Sustainable geothermal operation requires reinjecting the used thermal water into the reservoir. Otherwise, overexploitation may lead to a decline of reservoir pressure and production rates (Bálint and Szanyi 2015), compaction, land subsidence, and even induced seismicity (e.g., Seibt and Kellner 2003; Ungemach 2003; Békési et al. 2022). Currently, the produced water is discharged entirely in surface reservoirs (Szanyi et al. 2021). However, from 2027 all the produced thermal water must be reinjected into the subsurface by law (Mádl-Szőnyi et al. 2024). Therefore, there is a pressing need to find solutions to the commonly observed injectivity decline of injection wells targeting the UP sandstone formation.

Markó et al. (2021) provide a framework for identifying potential mechanisms leading to injectivity decline (and in some cases increase) in a sandstone aquifer over several spatial scales (Fig. 1). At local scale, clogging as a result of formation damage may occur depending on underlying physical processes such as sand migration (Rosenbrand et al. 2014). Other local processes are scaling, corrosion (Ochi and Vernoux 1998) and microbial pollution (Croese et al. 2019). At regional scale, low reservoir permeability and limited reservoir extent may play a role (Budai et al. 2024; Luo et al. 2023). Local effects may be more pronounced in loose, unconsolidated sandstone formations such as the UP sandstone. Using this framework, Brehme et al. (2024) have recently reported on the first application of thermal and chemical stimulation in UP sandstone in Mezőberény in South-Eastern Hungary to enhance injectivity drop in a geothermal well doublet. The treatment was designed based on a petrophysical characterization campaign (Willems et al. 2021). A comprehensive overview on the mechanisms causing injectivity decline and enhancement in geothermal projects is provided by Luo et al. (2023).

The risk of formation damage is also known for CO_2 storage, CO_2-based enhanced oil recovery, produced water re-injection (PWRI) and well killing in petroleum engineering, where foreign-fluid is injected in sedimentary (clastic or carbonate) reservoirs to prevent unintended fluid inflow into the wellbore, especially in formation with high permeability (Civan 2007; Martyushev et al. 2024; Zhao et al. 2025). However, if bottom-hole pressure exceeds reservoir pressure, deterioration of formation characteristics may occur, such as reduction in well skin, permeability, injectivity or productivity. Mechanisms leading to formation damage may include incompatibility between the injection fluid and pore fluid or rock, change in pore structure and the migration of fine particles (Luo et al. 2023). The latter is associated with the interaction of water phase with the swelling of clay minerals (particles) of the reservoir rock.

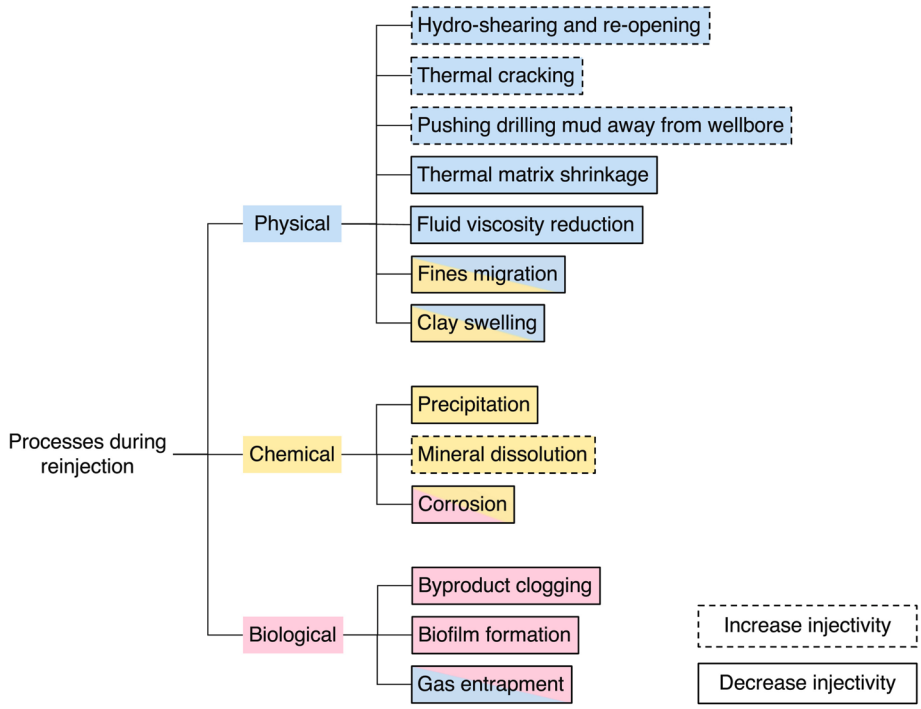


Fig. 1 Overview of mechanisms underlying injectivity decline and enhancement during reinjection. Mechanics are color-coded by type, i.e., whether they are physical, chemical or biological. Mechanisms in two colours include two processes, i.e., physico-chemical, physico-biological, chemo-biological processes (Luo et al. 2023)

The processes at local scale are often associated with near-wellbore area. Therefore, it has been proposed that low injectivity in sandstone rock formation can be overcome by the utilization of recompletion and selecting proper stimulation techniques from petroleum engineering (Economides and Nolte 2000). The most common stimulation techniques include chemical, hydraulic, mechanical and thermal methods. Chemical stimulations involve matrix acidizing, such as the removal of scale and screen plugging, acid washes and microbial treatment for biofilm removal (Portier et al. 2007; Markó et al. 2021). Hydraulic methods include hydraulic fracturing including gel-proppant fracs, hybrid fracs, water fracs and frac and pack or skin frac treatments as well as hydraulic shear stimulation (e.g., Zimmermann et al. 2010; Hofmann et al. 2019; Park et al. 2020). Mechanical methods cover re- and additional perforations (Nitters et al. 2016) as radial water jet drilling (Blöcher et al. 2016) and micro turbine drilling (Geissler et al. 2023). The main components of the hydraulic methods are a fracturing fluid consisting of water and proppants tailored to a specific stimulation design. The frac and pack and skin frac techniques have been applied for enhancing well performance in soft, unstable formations with high permeability in the petroleum industry worldwide since several decades (e.g., Roodhart et al. 1994; Morales et al. 2003). However, to the best of our knowledge, neither of the latter methods has been applied in geothermal wells because of economic reasons. The methods rely on creating a relatively short, highly conductive fracture in a reservoir to overcome near-wellbore damage (Roodhart et al. 1994). Frac and pack technique is performed with a screen and proppant, and subsequently gravel is

pumped behind the screen for formation integrity and preventing sand production after a propped frac is induced. Skin frac employs tip screen out fracturing design, pumping through perforations. The treatment design requires determination of the extent of formation damage (skin factor), petrophysical parameters of the formation as well as in-situ stress field.

The Hungarian national research and development project "Development of a well completion technology for sustainable and cost-effective reinjection of thermal water" (GINOP) was launched with the aim to develop tailored methodologies for sustaining the injectivity of geothermal wells in Upper Pannonian sandstone reservoirs with a focus on the Szentes geothermal field. The project includes petrophysical and geochemical characterization of UP sandstone formations as well as drilling and completion of a new reinjection well for the demonstration of long-term reinjection over 18 months. In this paper, we present the intervention in an existing production well for reinjection using various stimulation techniques to increase its injectivity. This includes the first application of the skin frac method in a geothermal well.

Site characterization

Geographical and geological setting

One of the most intensively utilized geothermal areas in Hungary is the Szentes geothermal field (Fig. 2), including the towns Szentes, Szegvár and Fábiensebestyén with 40 active wells producing more than 5.5 million m^3 of hot water annually with a total installed capacity of approx. 42 $MW_{thermal}$ and gross heat production in 2021 of approx. 32 GWh/year (Bálint and Szanyi 2015; EGEC Market Report 2023).

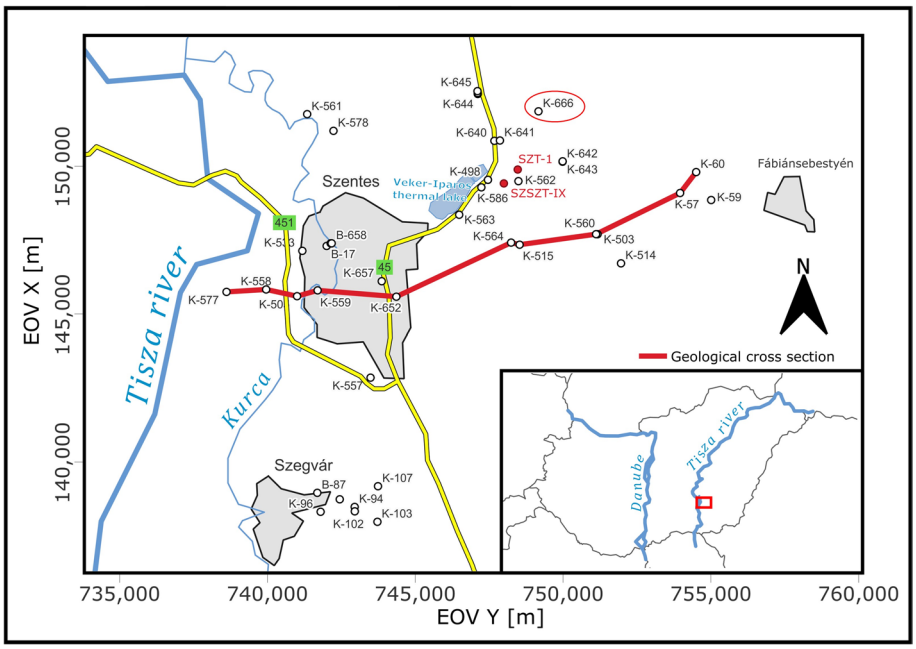


Fig. 2 Location of the study area in Hungary, showing the active producing geothermal wells of the Szentes geothermal field. The wells SZT-1 and SZSZT-IX were drilled, and well SZT-VIII (K-666) was recompleted in the framework of the GINOP project. The geological cross section across the field is shown in Fig. 3 (modified after Koroncz et al. 2022)

The latest study on the production history of the Szentes geothermal field was done by Bálint and Szanyi (2015) who review the field development and hydraulic characteristics, such as production history of the wells and the latest production test campaign conducted in 20 wells between 2009 and 2010. They observe continuous productivity decline over several decades. It is concluded that long-term production without reinjection results in regional pressure decrease in Upper Pannonian sandstone layers, which affects production well performance. There has been an attempt to improve the productivity of the wells by rationalizing well operation and applying longer shut-in periods, but these did not give satisfactory result. Figure 4 illustrates the geological setting in the study area including the characteristic formation (Fig. 4a) and the representative paleoenvironment (Fig. 4b). According to the geological characterization of the study area by Koroncz et al. (2022), the Szentes area is part of the northern wedging of the Makó trough, where the depth of the Pre-Neogene basement ranges from 3000 to 5000 m (Békési et al. 2022). Basin subsidence began in the Miocene, with the highest rate in the Pannonian (Late Miocene to Pliocene) resulting in sediment deposition with a thickness of at least 4000 m. From a lithostratigraphic point of view, the first group of sandstone formations is referred to as Tótkomlós Formation or marl that was formed in Mid-Miocene. After that Lower Pannonian (LP) sandstone formations were deposited. It comprises the Endrőd Formation, the Szolnok Formation and the Algyő Formation. These are characterized by layers of calcareous marl, clay-marl and very fine-grained powdered quartz sandstone in a deep basin environment as turbidites on a delta (shelf) slope. The younger Upper Pannonian (UP) sandstone formations are the Újfalu and Zagyva Formation. The lower part of which is characterized as sandstone with clay-aleurite streaks or laminae. These are the result of deposition in a delta or alluvial plain, moor and smaller bay environments. The upper 300–400 m of these sandstone layers are described as loose, poorly consolidated sandstone. The UP sandstone layers are covered by Pliocene and Pleistocene (terrestrial) sediments, such as sand, gravel, loess and clay. Note that according to the latest stratigraphic nomenclature, the Újfalu and Zagyva Formations are referred to as Dunántúli (Transdanubian) Formation Group, and the Tótkomlós, Endrőd, Szolnok and Algyő Formations are referred to as Alföld Formation Group (Koroncz et al. 2022). We use the term UP sandstone formation as lithofacies associations of Zagyva and Újfalu Formations in this study (Willems et al. 2021).

Geothermal reservoir characteristics

At the Szentes geothermal field, the production intervals of geothermal wells are mainly perforated in the Újfalu Formation at a depth of 1800–2500 m (Fig. 3 and Table 1). In the framework of the GINOP project, two new wells were drilled in 2020, SZSZT-IX and SZT-1 with several coring intervals for conducting a laboratory characterization campaign. Furthermore, well SZT-1 will serve as a demonstration well for conducting long-term reinjection experiments in the future. The existing production well SZT-VIII was temporarily repurposed for studying injectivity-related phenomena.

According to Koroncz et al. (2022), the UP sandstone formation in well SZT VIII is characterized as fine and medium sandstone intercalated by thin marl and siltstone layers. From a sedimentological point of view, the sandstone bodies exhibit an origin of estuary bar, delta branch river bed filling, and crevasse splay. The intercalating layers

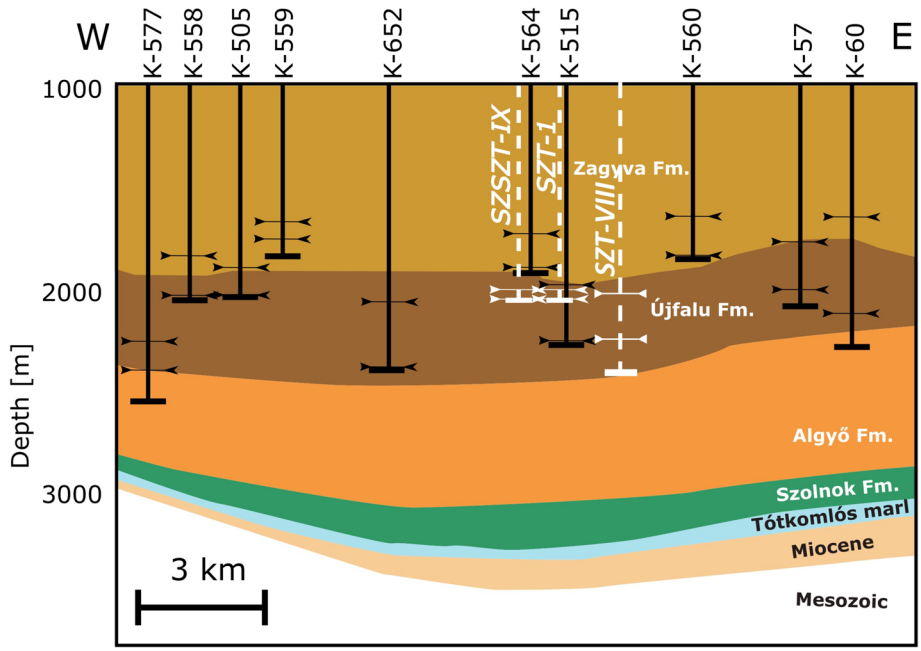


Fig. 3 Stratigraphic cross section across the study area illustrating well positions with top and bottom of production perforation interval. The section path is shown in Fig. 2. The wells SZT-1 and SZSZT-IX were drilled, and well SZT-VIII (K-666) was recompleted in the framework of the GINOP project (modified after Koroncz et al. 2022)

Table 1 Characteristics of wells located at the Szentes geothermal field close to the wells SZT-1 and SZSZT-IX as well as SZT-VIII (in bold) drilled and recompleted in the framework of the GINOP project, respectively. EOV Y and X stand for the geodetic coordinates of Hungarian maps (modified from Bálint and Szanyi 2015; and Koroncz et al. 2022)

Local Well ID	National well ID	EOV Y (m)	EOV X (m)	Drilling year	Depth (m)	Perforation Top–bottom (m)	Bottom-hole temperature (°C)	Production rate (m^3/year)
AL/1	K-561	741.347	151.764	1969	2050	1801–2019	85	256.000
AL/2	K-578	742.231	151.198	1971	2401	2135–2401	94	256.000
SZSZT-IX	K-707	747.995	149.416	2020	2009	1932–1997	88	–
SZT-1	K-712	748.464	149.886	2020	2000	1934–1981	93	–
SZT-I	K-498	747.458	149.539	1964	1995	1800–1975	85	154.860
SZT-II	K-562	747.489	149.493	1970	1800	1640–1793	82	150.850
SZT-III	K-563	746.484	148.355	1970	1992	1678–1936	78	170.150
SZT-IV	K-586	747.234	149.283	1972	2303	2060–2235	96	178.604
SZT-V/1	K-640	747.855	150.857	1979	2240	2040–2210	94	134.800
SZT-V/2	K-641	747.800	150.800	1979	2000	1785–1993	84	155.100
SZT-VI/1	K-642	749.981	150.148	1978	2398	2046–2255	97	172.500
SZT-VI/2	K-643	749.982	151.063	1978	1998	1694–1989	86	189.000
SZT-VII/1	K-644	747.112	152.442	1979	2257	2053–2205	96	156.900
SZT-VII/2	K-639	747.111	152.480	1979	1806	1534–1754	76	174.300
SZT-VII/3	K-645	747.101	152.539	1980	1998	1800–1998	80	194.100
SZT-VIII	K-666	749.166	151.854	1988	2261*	1998–2137	90	128.900

* Accessible depth

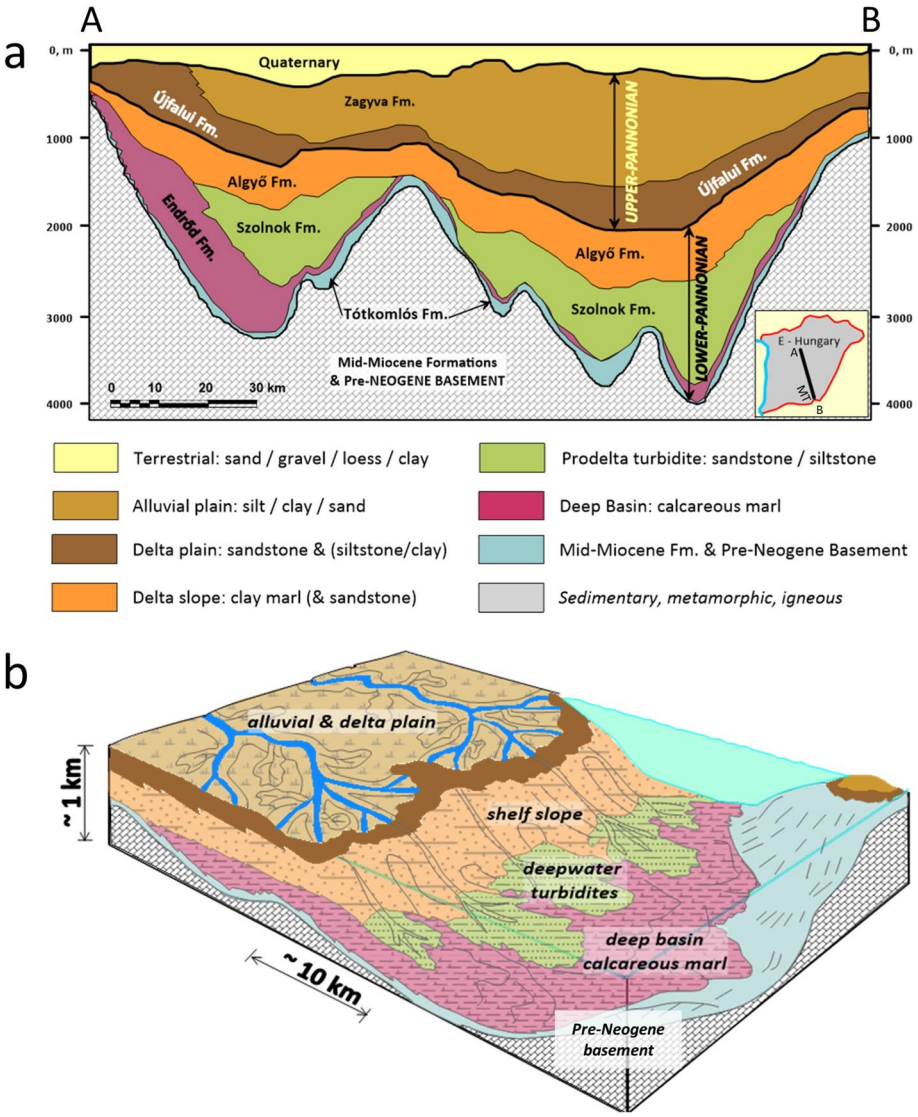


Fig. 4 Cross section of the Great Hungarian Plain illustrating characteristic geological formations (**a**); and sedimentological block diagram illustrating the Late Miocene paleoenvironment (**b**). MT stands for Makó trough (modified from Almási 2001 and Njeru et al. 2024b)

may be associated with an oxbow lake environment. The UP sandstone samples from wells SZT-1 and SZSZT-IX consist of mainly quartz, dolomite and calcite (carbonates), albite as well as clay minerals, such as montmorillonite and kaolinite (Table 2). According to Njeru et al. (2024a) micro-CT analyses conducted on UP sandstone samples identify generally weak cementation and the presence of fine-grained materials in smaller pores.

Figure 5 shows the classified sediments in Újfalu Formation samples obtained from well SZT-1. According to Koroncz et al. (2022) the samples contain a significant ratio (over 50%) of fine sediments, such as clay, silt, very fine and fine sand, whereas the ratio of medium and coarse sand varies between 1 and 35%. This is also reflected in Fig. 6 which shows the grain size distribution on water samples obtained from well SZT-VIII

Table 2 Average mineral composition of Upper Pannonian sandstone formation samples based on XRD measurements (Koroncz et al. 2022)

Mineral phase	Average mass fraction (%)
Calcite	3.53
Quartz (alpha)	52.59
Microcline	7.98
Albite (low)	10.56
Kaolinite	5.43
Dolomite	12.91
Montmorillonite (MgCa)	4.85
Clinochlore	2.15

prior to stimulation experiment. The distribution is determined for grains taken from surface screen and fine sediments in the brine. According to Table 3, the former exhibits very fine sand as fine content (D10) and medium sand as coarse particle (D60), while the fine content is clay, with D60 representing silt in brine. This has implications for potential fines and particle migration. Coarser particles tend to deposit and will not mobilize after deposition, resulting in potential clogging in the reservoir. On the other hand, fine particles may remobilize after deposition, as long as fluid flow velocity exceeds the critical velocity (Zhang et al. 2022).

The petrophysical parameters are summarized in Table 4 based on several laboratory experiments including grain density, porosity, permeability, clay, silt and sand content as well as strength and elastic parameters reported by Koroncz et al. (2022) and Gelencsér et al. (2022), respectively. The core samples were obtained during drilling of wells SZT-1 and SZSZT-IX in 2020 from depth intervals between 1740 and 1972.5 m with an average core recovery of approx. 85% (Koroncz et al. 2022). The petrophysical parameters show a strong dependence on diagenetic features such as grain size, clay content, rock fabric and layering which is reflected in relatively high standard deviation compared to the average value in Table 4. Furthermore, clay content shows an inverse relationship with porosity and permeability, and a positive correlation with strength values. The Mohr–Coulomb parameters cohesion and angle of internal friction, determined from multiple failure state tests in triaxial compression (Kovári test), demonstrate either only compaction without shearing or shear enhanced compaction. This implies considering pressure-dependent elastic moduli (Young's modulus and Poisson's ratio) for which the stress–strain curves are provided in Gelencsér et al. (2022).

Table 5 summarizes the typical composition of geothermal brine in the Újfalu Formation sampled from well SZT-V/2 close to well SZT-VIII. The composition exhibits sodium–HCO_3-type geochemistry with low salinity (TDS < 5000 mg/l) of paleometeoric origin characteristic for fine grained Late Miocene to Pliocene sediments in formations of the Great Hungarian Plain in Hungary (Varga et al. 2019).

History of injection-related issues in geothermal systems

Low injectivity is often experienced in geothermal doublets installed in sandstone reservoirs (Markó et al. 2024). For example, the Mezőberény site, which is located

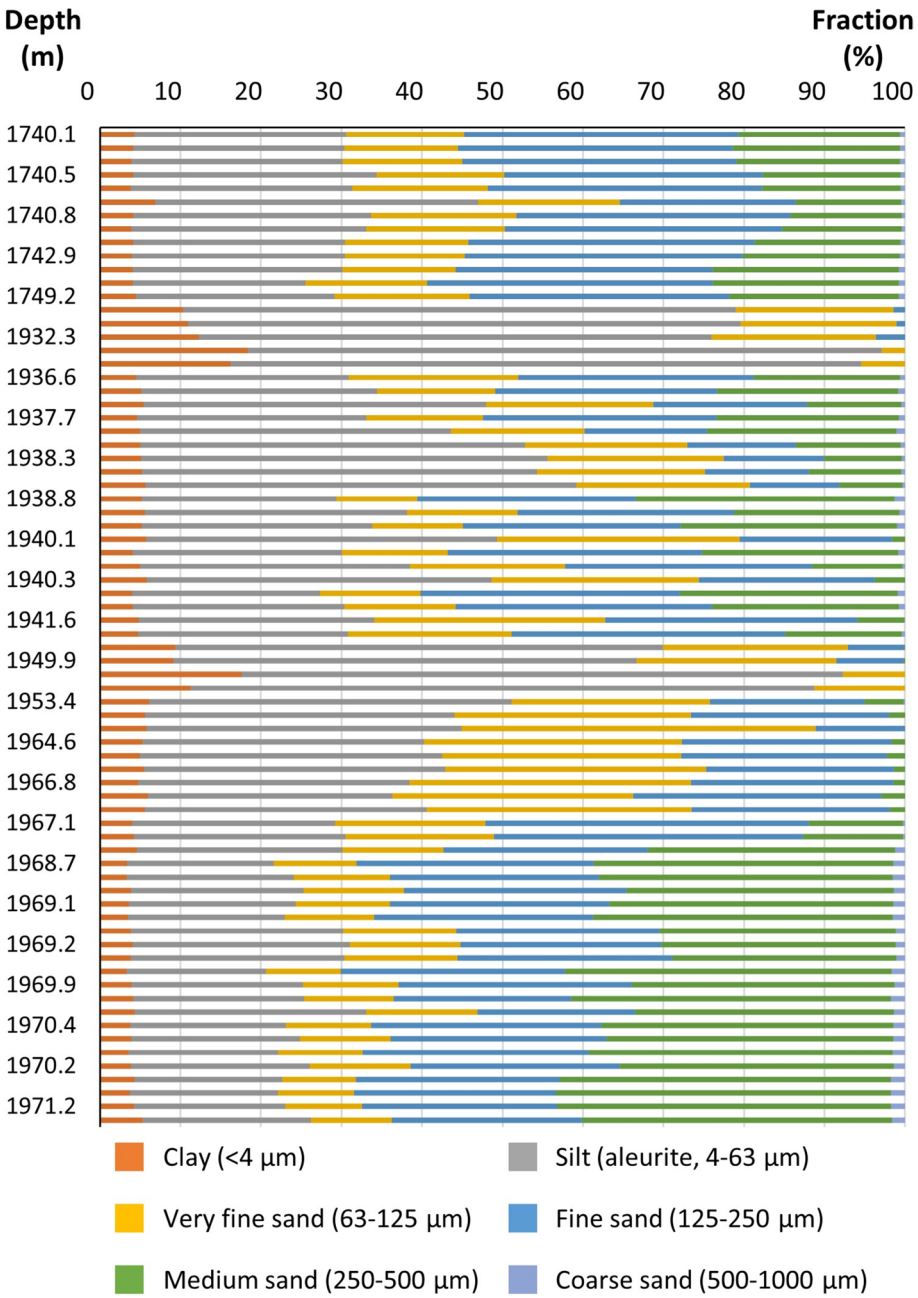


Fig. 5 Categorisation of sediments in well SZT-1 with depth based on the Udden-Wentworth scale. The top of the Upper Pannonian Újfalu sandstone formation is at a depth of 1932 m (modified after Gelencsér et al. 2022)

approx. 80 km east to the present study site in southeastern Hungary, and it has perforation intervals in the Újfalu formation, is reported to exhibit strong injectivity decline of one order of magnitude within 1 month of operation in 2012–2013. Markó et al (2021) point out that the phenomenon could be related to insufficient transmissibility of the geological reservoir as well as pore throat blocking and skin in the near-wellbore area as a result of chemical or mechanical clogging processes.

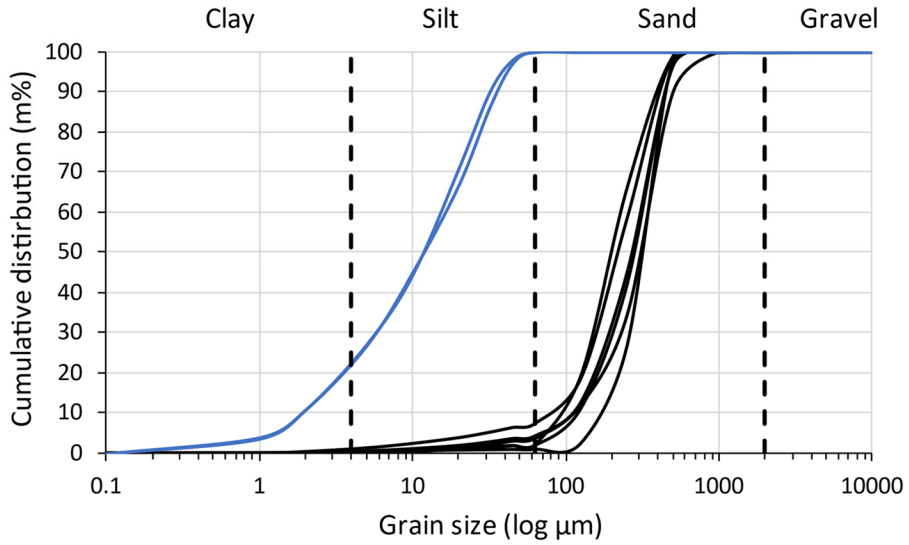


Fig. 6 Grain size distribution of brine samples obtained from well SZT-VIII prior to stimulation in 2020. The black curves represent samples taken from surface screen, and blue lines represent fines in brine

Table 3 Grain size distribution of samples obtained from well SZT-VIII according to Fig. 6

Cumulative grain size distribution category	6 samples taken from sand screen in brine sampling tank, average ± std. deviation (µm); grain class	2 brine samples, average ± std. deviation (µm); grain class
D10	90 ± 40; very fine sand	1.8 ± 0; clay
D60	300 ± 50; medium sand	15 ± 1; silt

Table 4 Summary of petrophysical and mechanical parameters of the Upper Pannonian sandstone formation

Parameter	Average value	Standard Deviation	Comment
Depth (m)	1882	93.5	121 tested samples from wells SZSZT-IX and SZT-1 (Koroncz et al. 2022)
Grain density (kg/m^3)	2710	15	
Porosity (%)	27	6	
Permeability (m^2)	7 10^{-13}	6 10^{-13}	
Clay and fine silt content (%)	16.9	8.2	
Sand content (%)	42.3	20.9	
Uniaxial compressive strength (UCS, Pa)	1.2 10^7	1.5 10^7	26 samples from well SZT-1 (Gelencsér et al. 2022)
Young's modulus (Pa)	6.1 10^9	6.9 10^9	
Poisson's ratio (–)	0.24	0.08	
Brazilian Tensile Strength (BTS, Pa)	7 10^5	9 10^5	24 samples from well SZT-1 (Gelencsér et al. 2022)
Cohesion (Pa)	8.9 10^6	4.4 10^6	23 samples from well SZT-1 (Gelencsér et al. 2022)
Angle of internal friction (°)	32	3.8	

Methods

Evaluation of well and near-wellbore conditions

Based on availability, production history, perforation interval length and the static

Table 5 Representative ion composition of geothermal brine in the Újfalu Formation sampled from well SZT-V/2

Ca^{2+} (mg/l)	K^{+} (mg/l)	Mg^{2+} (mg/l)	Na^{+}(mg/l)	Fe (total) (mg/l)	Cl^{-}(mg/l)	SO_4^{2-} (mg/l)	HCO_3^{-}(mg/l)	CO_2(mg/l)	TDS (mg/l)	pH
5.44	10.9	1.04	596	0.2	8	5	1629	54	2310	8.0

geological and hydrogeological model of the study area, well SZT-VIII was selected for the intervention. However, the state of the well and the near-wellbore conditions had to be characterized due to historical nature of available data. Therefore, well integrity had to be determined by assessing the casing, cement quality and sand screens. The well logging campaign included Caliper, Radial Bond Logging (RBL), Natural Gamma Ray and resistivity measurements.

After gaining confidence in adequate well integrity, injection tests were conducted to estimate the baseline hydraulic characteristics of the well, such as transmissibility (permeability), skin and injectivity index.

Temperature and flow meter logs were used to determine the contribution to overall flow of each screen section, where temperature logging is conducted prior to and after the cold-water injection to obtain differential temperature profile. Differential temperature was calculated by averaging the temperature decrease across the perforations and dividing that by the average of the baseline temperature profile before injection. By analyzing the temperature logs run after the injection, inflow zones can be identified qualitatively, which are indicated by a negative temperature anomaly. It can be assumed that the higher the temperature change, the more fluid can be injected into the interval. The flow meter was equipped with quartz transducers to provide flow profile, temperature, opacity and electrical conductivity logs.

The well test analysis was conducted using pressures recorded by downhole memory tool at 1950 m MD and flow rates. Absolute pressures are converted to differential pressures, where the initial pressure is set to zero. The analysis of the well properties, such as permeability, transmissivity and skin, was done by application of type curve analysis using the software package Saphir (Kappa Engineering).

The evolution of transmissivity and skin is calculated from decline pressure curves during and after the last injection stage taking into account the superposition principle and assuming infinite acting radial flow (Horne 1995). The calculations are based on the generalized formula for pressure development with stepwise flow rate changes:

$$p(r,t) = p_0 + \sum_{i=1}^{n} \frac{(q_i - q_{i-1})\mu}{4\pi kh} \times (0.5772 + \ln\left(\frac{\varphi\mu c_t r^2}{4k(t-t_{i-1})}\right) - 2s) \tag{1}$$

with p(r,t), well pressure; p_0, initial pressure; h, interval length (height of reservoir); k, rock permeability; q_i, flow rate at i^{th} interval i; μ, dynamic viscosity of fluid; γ, 0.5772 (Euler constant); t_i, interval time i; t, total time; ϕ, porosity; c_t, total compressibility; r, well radius; s, skin.

The transmissivity (k h) is calculated from the logarithmic superposition time derivative of the pressure decline curve based on Lee (1982):

$$\frac{\partial(\Delta p)}{\partial(\ln(\frac{t_s}{t_s+t_p}))} = \frac{q\mu}{4\pi kh} \tag{2}$$

where t_s is the shut-in time and t_p is the injection time.

In addition to these, the injectivity index (*II*) is calculated as the ratio of injection rate and downhole pressure increase, *DHP* at the end of the highest injection rate phase during each injection test:

$$II = \frac{q}{DHP} \tag{3}$$

Decision on the stimulation program

Possible problem sources were investigated using the generalized concept introduced by Markó et al. (2021). Based on that case study, which was applied on the Mezőberény site with reservoir characteristics similar to the study area, such as lithostratigraphy, brine composition and well completion, the potential injectivity decline in UP sandstone rock can be associated with reservoir characteristics, i.e., low transmissibility, or with near-wellbore phenomena, such as mineral precipitation or local particle migration. Consequently, hydraulic fracturing, chemical (acid) treatment, as well as skin frac experiment were considered.

The motivation behind hydraulic fracturing is its possibility to enhance the permeability or transmissibility of an interval with low reservoir permeability. Chemical stimulation may be used to dissolve precipitated minerals, e.g., scales at perforations. Skin frac method may enhance both near-and far-field wellbore hydraulic parameters. The effect of these interventions was evaluated by well test analysis of injection tests after each treatment.

Since all injection-related problem sources associated with permeability and formation damage were considered with the highest probability compared to mineral precipitation due to relatively low TDS content in brine, thus, hydraulic fracturing and skin frac experiment were prioritized originally. By performing hydraulic fracturing first, final design for skin frac test can be made. However, due to operational reasons, acid treatment preceded skin frac experiment.

The skin frac treatment was designed using a commercial software that employs a pseudo-3D hydraulic fracturing model to compute fracture dimensions (FracPro, Cleary 1994). It can be used to predict the pressure response in the well and to select the appropriate equipment. A tensile fracture (mode I) opening perpendicular to the minimum principal stress is assumed.

Results

Experimental design

The schematic structure of the recompleted vertical well SZT-VIII is provided in Table 6 and Fig. 7. The perforated intervals are summarized in Table 7. Note that the well has a drilling true vertical depth of 3400 m, and a bottom casing depth of 2893 m, but the well bottom is filled with a cement plug until 2605 m.

Table 6 Casing string of well SZT-VIII

Casing string no	Diameter (mm)		True vertical depth (m)	
	Outer	Inner	Top	Bottom
1	473 (18 5/8″)	–	0.0	45.5
2	340 (13 3/8″)	318 (12 5/8″)	0.0	493.0
3	244 (9 5/8″)	228.5 (8 7/8″)	0.0	1793.0
4	178 (7″)	159.4 (6 1/4")	700.2	2893.0

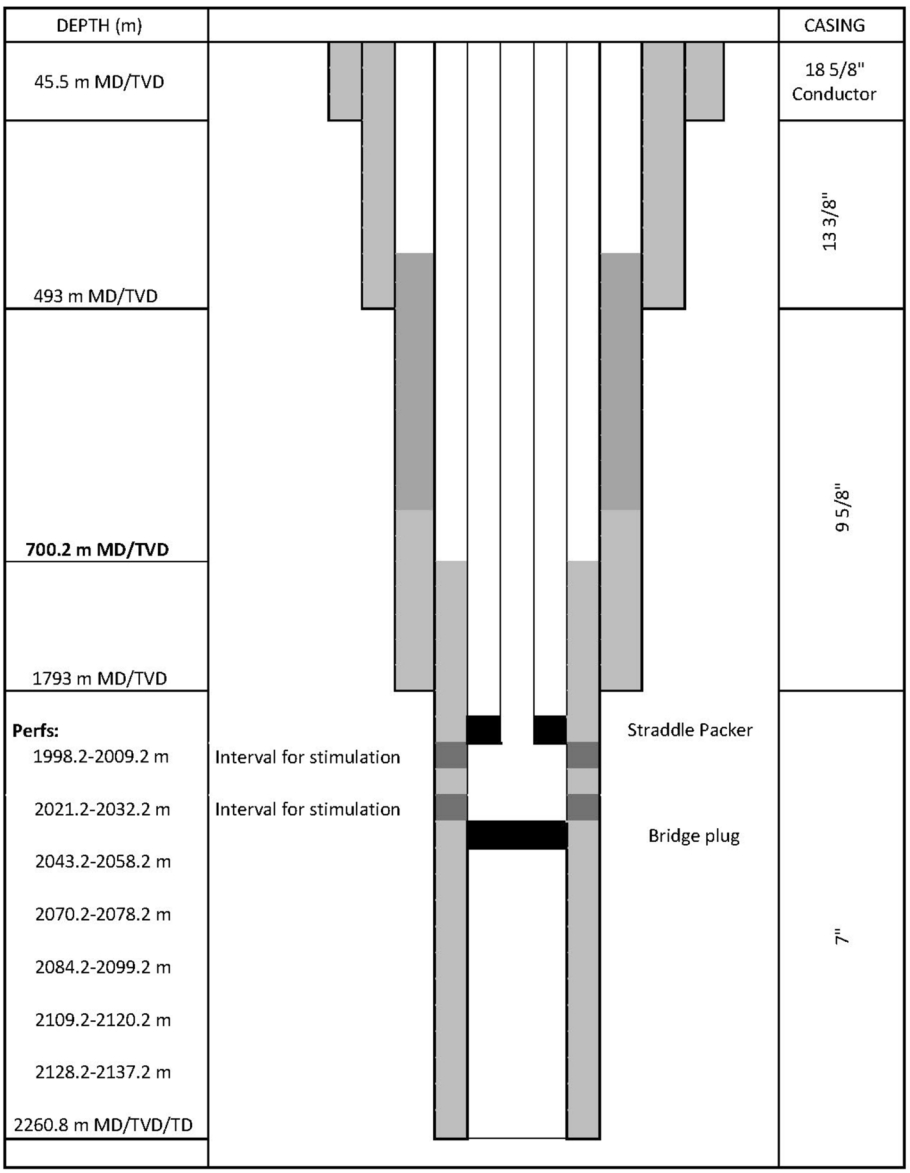


Fig. 7 Schematic illustration of tested well SZT-VIII. The total depth (TD) corresponds to accessible depth (Table 1). The experimental setup reflects conditions for skin frac experiment (Test #11 in Table 8)

Table 7 Perforation intervals of well SZT-VIII

Perforation No	True vertical depth from – to (m)	Length (m)
I	1998.2–2009.2	11
II	2021.2–2032.2	11
III	2043.2–2058.2	15
IV	2070.2–2078.2	8
V	2084.2–2099.2	15
VI	2109.2–2120.2	11
VII	2128.2–2137.2	9
Total length of perforations		80

Based on cement bond logs the well cement is in an acceptable condition for intervention despite several locations, where it is in moderate or bad condition. The logs also reveal that the accessible depth is only 2260.8 m due to sand debris and cement spalling. At this depth the bottom-hole temperature is 115.2 °C. There is hint towards moderate mineral precipitation.

The intervention is realized on the basis of hydraulic tests. Injection water is provided from nearby wells SZT-V/1 (K-640), SZT-V/2 (K-641) and SZT-VII/2 (the location of well K-639 coincides with well K-644 in Fig. 2). During the tests, downhole pressure and temperature were monitored with a probe installed at a depth of 1950 m, above the top of the first perforation interval. The downhole flow rate is recorded using a flow meter to determine the inflow rate of the tested perforation interval.

First, injection tests to determine reservoir permeability were conducted on all perforation intervals at once (Test #1). All well tests in this study are realized by injection tests with several pressure build ups with subsequent shut-in phase. These are repeated several times while increasing the injection rate gradually. This test is followed by investigating a single perforation interval with the highest flow rate and permeability to understand the near- and far well characteristics of the well-performing interval (Test #2). This required the isolation of the target interval by installing a bridge plug below and by inflating a straddle packer above that interval. Permeability determined from this test can serve as a reference value for subsequent tests. Further tests were conducted with the same bridge plug and packer setup. The reference well test was followed by a step-rate test using water (Test #3 and #4). After that hydraulic fracturing was conducted using gel and proppant followed by another well test (Test #5 and #6). These tests were followed by acid treatment and injection test (Test #7 and #8) as well as unplanned pump lift (Test #9) and injection test (Test #10), which are presented in the Results section. Using these test results, the skin frac test with tailored fracturing fluid and proppants was conducted based on a stimulation design developed using a commercial hydraulic fracturing simulator FracPro (Test #11a–c). For this treatment, both poor- and well-performing perforation intervals I and II, respectively, are included to mimic conditions similar to Test #1 (Fig. 7). The effect of each stimulation test is evaluated by injection tests (Test #12).

In total, 12 tests were conducted in well SZT-VIII in the framework of this study (Table 8). Ten of them were performed in 2020, while the skin frac test including preparatory injection and step-rate tests and the subsequent injection test were conducted in 2021. An overview of the field experiments is given in Table 8. Table 9 gives an overview of the change in well parameters, such as reservoir permeability and transmissivity, skin factor as well as injectivity index between the experiments. Figure 8 summarizes the results of the conventional well test analysis of the injection tests.

First injection test

First, water was injected in all perforation intervals at a total length of 140 m in several pressure build-up and fall-off (shut-in) phases to get an understanding of the hydraulic characteristics of the well (Fig. 9). Pressure and temperature were measured above the perforation intervals. Since water with surface temperature was injected into a hot reservoir there was a temperature difference of about 30 °C downhole with respect to

Table 8 Summary of hydraulic tests conducted in well SZT-VIII

Test No	Test	Description	Date
#1	Injection test 1	All perforation intervals are tested	08.05.2020–12.05.2020
#2	Injection test 2	Injection test in best performing perforation interval II, other perforation intervals are kept isolated until Test #10	23.05.2020–24.05.2020
#3	Step-rate test 1	Diagnostic test for assessing non-linear flow behavior	24.05.2020
#4	Injection test 3	Determination of possible change in well parameters	24.05.2020–25.05.2020
#5	Hydraulic fracturing	Hydraulic fracturing conducted with gel and sand-proppant	28.05.2020
#6	Injection test 4	Determination of permeability hindered due to pump failure	28.05.2020–29.05.2020
#7	Acid treatment	Acid washing for removing the injected gel and sand-proppant in the near-well area	03.06.2020
#8	Injection test 5	Determination of possible change in well parameters	04.06.2020–08.06.2020
#9	Pump lift	Water production for permeability enhancement	09.06.2020–12.06.2020
#10	Injection test 6	Determination of possible change in well parameters	13.06.2020–16.06.2020
#11a	Injection test 7	Preparatory test for skin frac experiment. Intervals I and II are stimulated in the remaining stimulation program	30.06.2021
#11b	Step-rate test 2	Preparatory test for skin frac experiment	
#11c	Skin frac experiment	Skin frac experiment with gel and bauxite-proppant	
#12	Injection test 8	Determination of possible change in well parameters on poor-performing interval I and well-performing interval II	03.07.2021–07.07.2021

initial reservoir fluid temperature. Thus, pre- and post-test conditions are evaluated using temperature, flow resistance, flow meter as well as fluid transparency (borehole televiewer) logs. The perforation interval performance is determined using an injection rate of 10 l/s. Figure 10 and Table 10 show that fluid enters the reservoir dominantly, i.e., more than 80% of the injection fluid rate, through the perforation interval II. This suggests that injectivity is controlled by this interval, where the vertical difference between the top depth of interval I and the bottom depth of interval II is 34 m. However, to incorporate inflow into the rest of the intervals as well, the reservoir thickness for the well test analysis is assumed to be larger, i.e., 46 m. The calculated permeability and transmissibility are 1.51 10^{-12} m^2 (1510 mD) and 3.72 10^{-11} m^3, respectively, and the injectivity index is 3.7 l/(s bar). The well shows a strong positive skin of over 6, which is a hint towards poor near-wellbore performance.

Second injection test

Based on first injection test, most of the injected fluid is absorbed by perforation interval II with large skin factor. Thus, prior to the second hydraulic test, a cement plug was installed at a depth of 2037.8 m, below perforation interval II and a straddle packer was inflated at a depth of 2016.5 m above that to isolate interval II from the other intervals for the study of injection-related phenomena in UP sandstone. Water was injected in the original tubing string. The injection test on perforation interval II with a length of 11 m reveals a reservoir permeability of 3.06 10^{-12} m^2 (3060 mD), transmissibility of 3.37 10^{-11} m^3 as well as strong negative skin of -5.2 (Fig. 11). The injectivity index is 4.1 l/(s bar). These test results serve as reference values for the subsequent experiments.

Table 9 Summary of results of the injection tests conducted in well SZT-VIII based on well test analysis. Following further input parameters are used well radius: 0.089 m, porosity: 27%, total compressibility: 4.35 10^{-10} 1/Pa

Test no	Effective interval length (m)	Test phase	Dynamic viscosity (Pa s)	Permeability (m^2)	Transmissibility (m^3)	Skin (–)	Injectivity index, *II* (l/(s bar))	Comment
#1	46	Shut-in	4.32 10^{-4}	1.17 10^{-12}	5.40 10^{-11}	6.21	3.7	All perforations are tested during injection test (Fig. 8)
		Injection		1.85 10^{-12}	2.04 10^{-11}	–		
#2	11	Shut-in	4.32 10^{-4}	4.05 10^{-12}	4.45 10^{-11}	− 5.16	4.1	Perforation II is tested during injection test (Fig. 10)
		Injection		2.08 10^{-12}	2.29 10^{-11}	–		
#4	11	Shut-in	4.32 10^{-4}	4.14 10^{-12}	4.55 10^{-11}	8.94	3.6	Perforation II is tested after step-rate test 1 (Fig. 13)
		Injection		4.53 10^{-12}	4.98 10^{-11}	–		
#8	11	Shut-in	4.32 10^{-4}	7.15 10^{-12}	7.86 10^{-11}	20.00	0.4	Perforation II is tested after acid injection (Fig. 15)
		Injection		7.72 10^{-13}	8.49 10^{-12}	–		
#10	11	Shut-in	4.32 10^{-4}	2.71 10^{-12}	2.98 10^{-11}	− 6.67	5.6	Perforation II is tested after pump lift (Fig. 17)
		Injection	4.32 10^{-4}	3.54 10^{-12}	3.89 10^{-11}	–		
#11c	11	Shut-in	5 10^{-1}	1.07 10^{-11}	1.18 10^{-10}	− 2.61	–	Perforation I and II are tested during skin frac test (Fig. 23)
#12	11	Shut-in	4.32 10^{-4}	3.36 10^{-12}	3.70 10^{-11}	6.02	3.6	Perforation I and II are tested after skin frac test (Fig. 23)

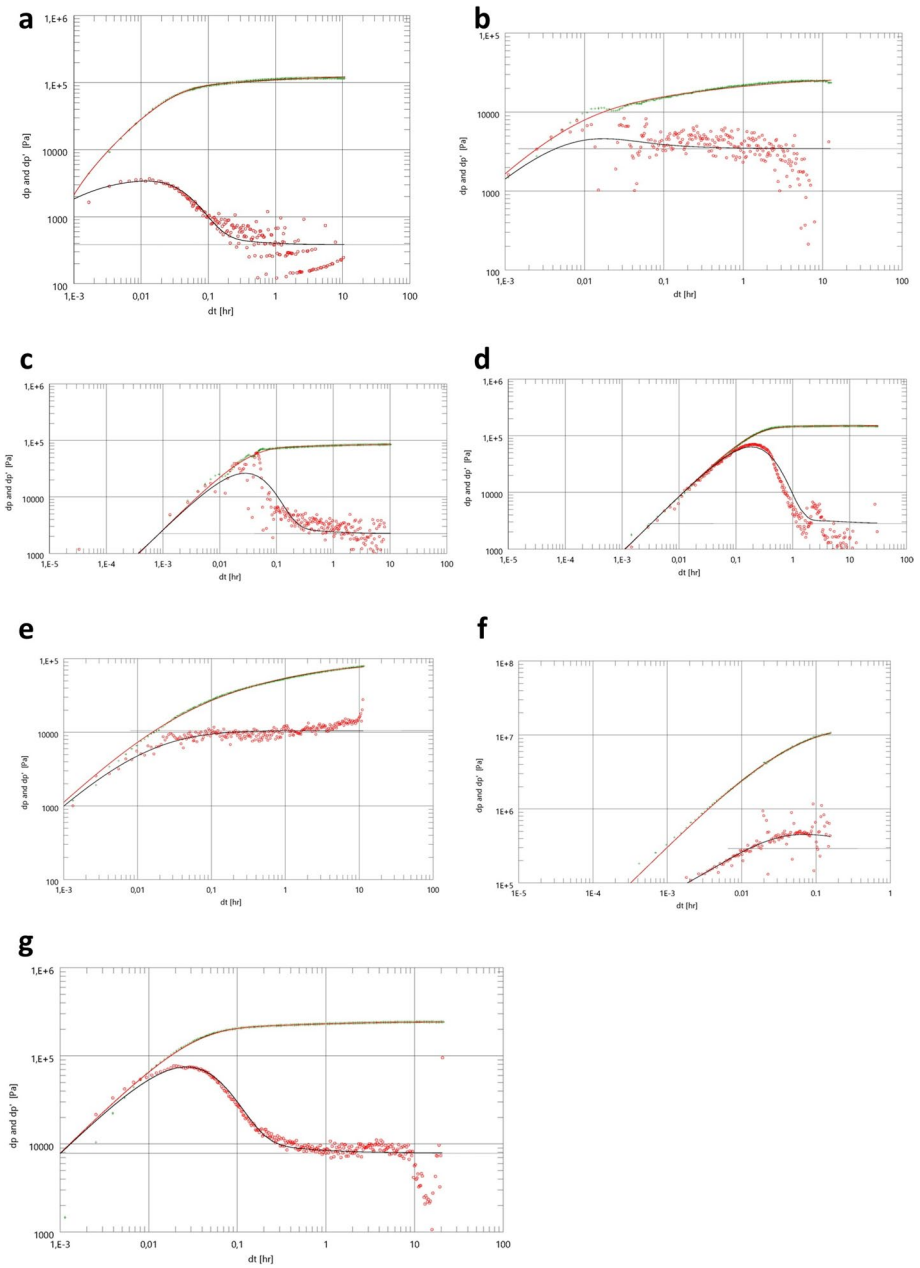


Fig. 8 Log–log plots of conventional well testing analysis with pressure (dp) and pressure derivative (dP') curves over time since stat of shut-in. Data points indicate field data; lines show fitted model results. **a** Test #1, **b** Test #2, **c** Test #4, **d**) Test #8, **e**) Test #10, **f**) Test #11c and **g**) Test #12

First step-rate injection test and third injection test

The step-rate test (Test #3) was conducted with water (Fig. 12). The aim of this experiment was to determine the pressure level at which a change in injectivity might be observed as indication for non-linear flow regime prior to hydraulic fracturing. The flow rate levels were 2.8, 4, 7.8, 11.8 and 13.3 l/s.

Figure 13 shows the injection rate—pressure evolution of the test which is based on average wellhead pressure at each flow rate step. According to that, non-linear behavior

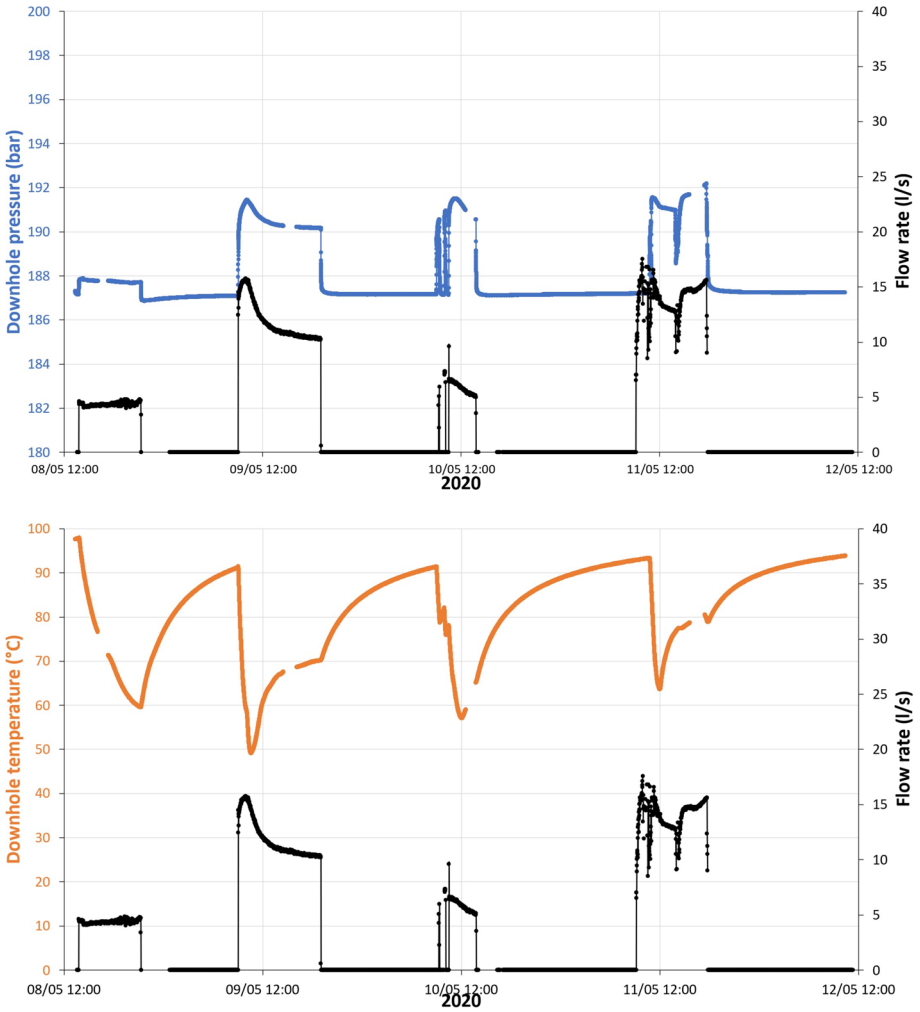


Fig. 9 Downhole pressure (top) and temperature (bottom) recorded at a depth of 1950 m as well as injection rate during the first injection test over all perforation intervals

may be observed between 7.8 l/s and 13.3 l/s and between 80 and 85 bar wellhead pressure, respectively. However, the transition is not unambiguous. This implies that hydraulic fracturing would require pumping at higher injection rates. The subsequent third hydraulic test reveals a permeability of 4.33 10^{-12} m^2 (4330 mD), a transmissibility of 4.77 10^{-11} m^3 and an injectivity index of 3.6 l/(s bar) (Fig. 14).

1st stimulation experiment: hydraulic fracturing and fourth injection test

Hydraulic fracturing (Test #5) was conducted using gel and sand as proppant. In total 8 m^3 of gel was prepared in a batch mixer at the injection site. The material parameters for creating the gel are summarized in Table 11. The gel was designed for a drying rate of 0.17 ml/s, pH of 10.3 and marsh viscosity of 180 s/l based on previous experience in commercial operation in an offset oil and gas well. Unfortunately, no flow rate records are available. The test was conducted on 28.05.2020 as follows (Fig. 15):

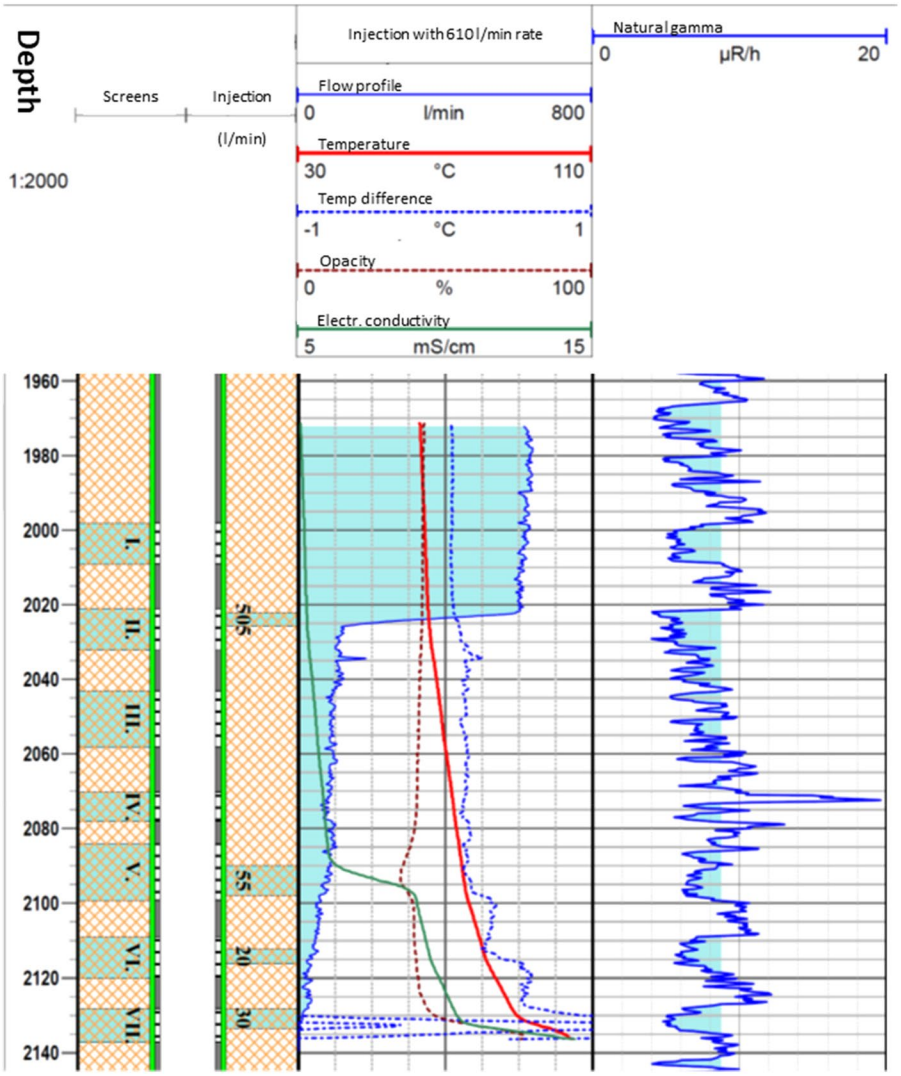


Fig. 10 Geophysical logs during an injection test of 610 l/min (10 l/s) with injection rate share of respective perforation interval in well SZT-VIII

Table 10 Perforation intervals of well SZT-VIII, performing intervals as well as flow rate based on injection test

Perf. Interval	Diameter (mm)		Depth (m)		Interval length (m)	Injection rate	
	outer	inner	Top	Bottom		(l/s)	(rel. %)
I	177.8 (7″)	159.4 (6¼″)	1998.2	2009.2	11	–	–
II			2021.2	2032.2	11	8.4	82.8
III			2043.2	2058.2	15	–	–
IV			2070.2	2078.2	8	–	–
V			2084.2	2099.2	15	0.9	9.0
VI			2109.2	2120.2	11	0.3	3.3
VII			2128.2	2137.2	9	0.5	4.9

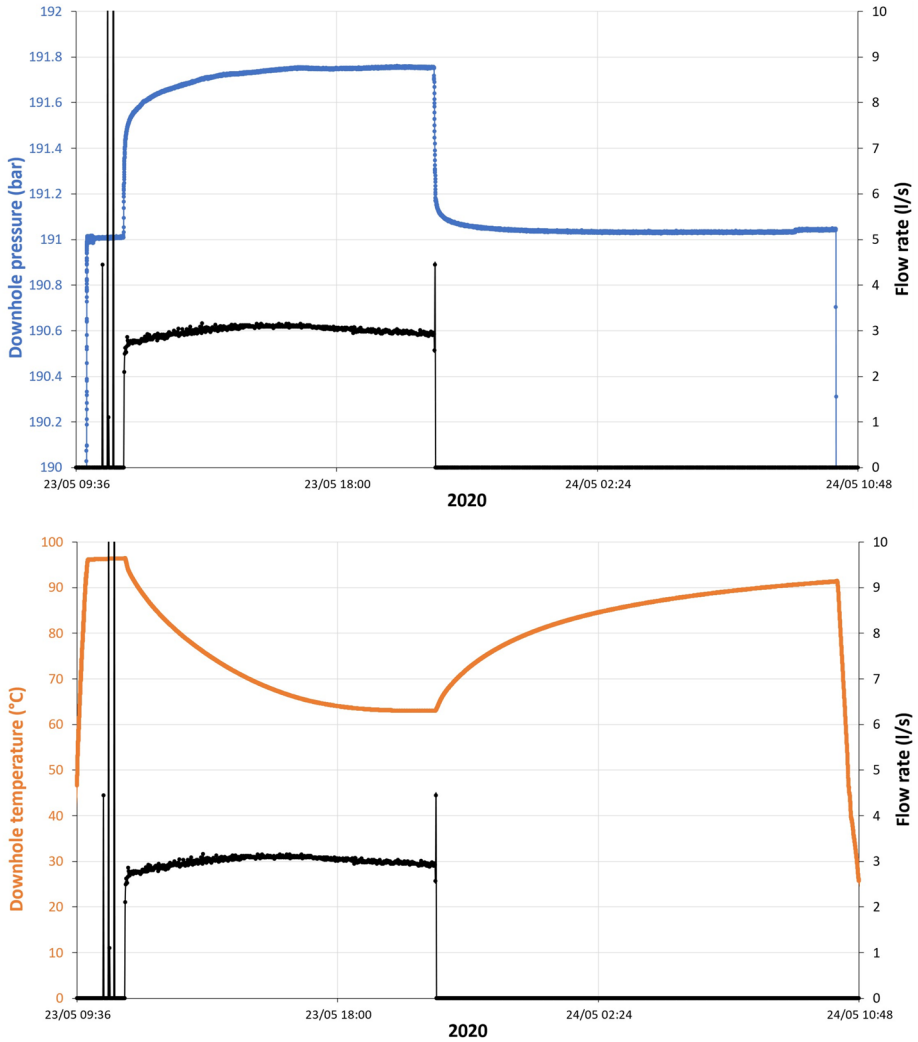


Fig. 11 Downhole pressure (top) and temperature (bottom) recorded at a depth of 1950 m as well as injection rate during the second injection test over the isolated perforation interval II

- Step 1: 12:25–13:05: Pure water injection in several steps;
- Step 2: 13:05–15:55: Mixing 8 m^3 gel into injection system;
- Step 3: 16:10–16:15: Injection of 2 m^3 gel at well-head pressure of 16 bar at 3.3–4.2 l/s flow rate;
- Step 4: 16:15–16:30: Injection of 6 m^3 water for settling;
- Step 5: 16:30–17:50: Preparation for hydraulic fracturing experiment. 17:30–17:50 Gel and proppant mixing.
- Step 6: 17:50–18:25: Gel and sand injection at 2.5–5 l/s rate and at max well-head pressure of 8 bar;
- Step 7: 18:25–19:30: Injection of 6 m^3 water for gel and proppant settling. First 3 m^3 of water is injected until the well-head pressure equilibrates at 150 bar. After that 3 m^3 of water is injected at 0.8–1.2 l/s rate with well-head pressure = 100–120 bar.

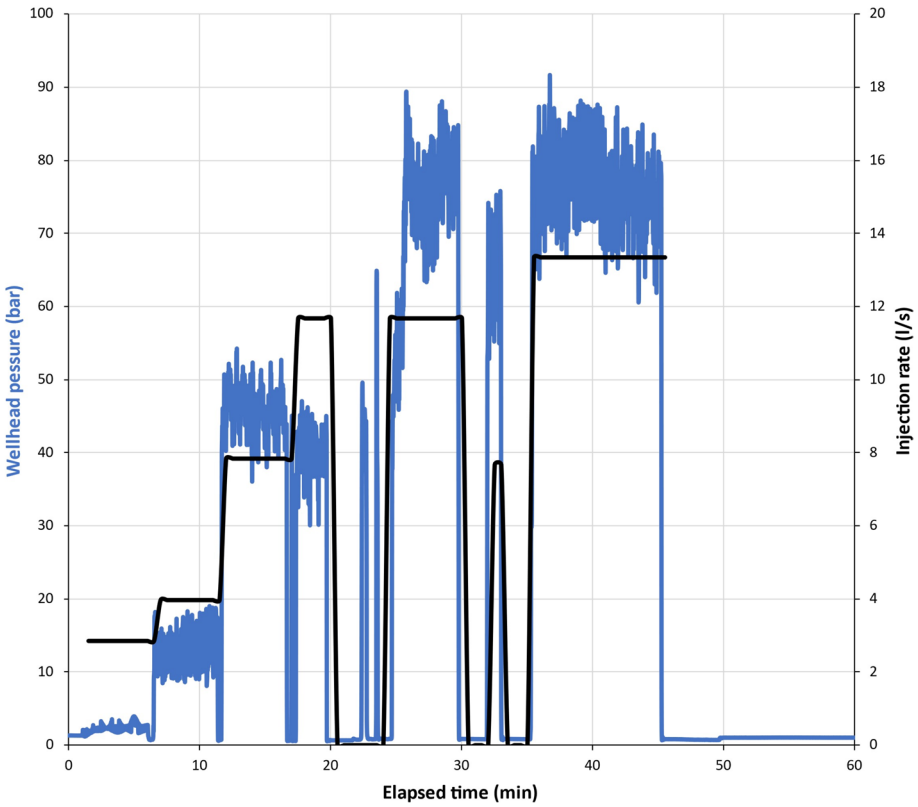


Fig. 12 Wellhead pressure and averaged injection rate during the step-rate test in the isolated perforation interval II

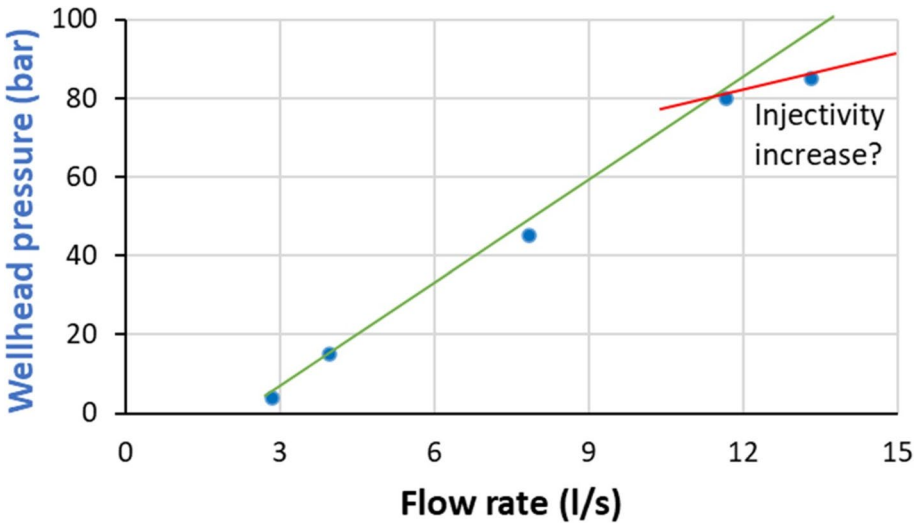


Fig. 13 Pressure vs flow rate plot based on the step-rate test shown in Fig. 12

The subsequent, fourth injection test was unsuccessful due to pump failure. This hinders evaluating the effect of hydraulic fracturing.

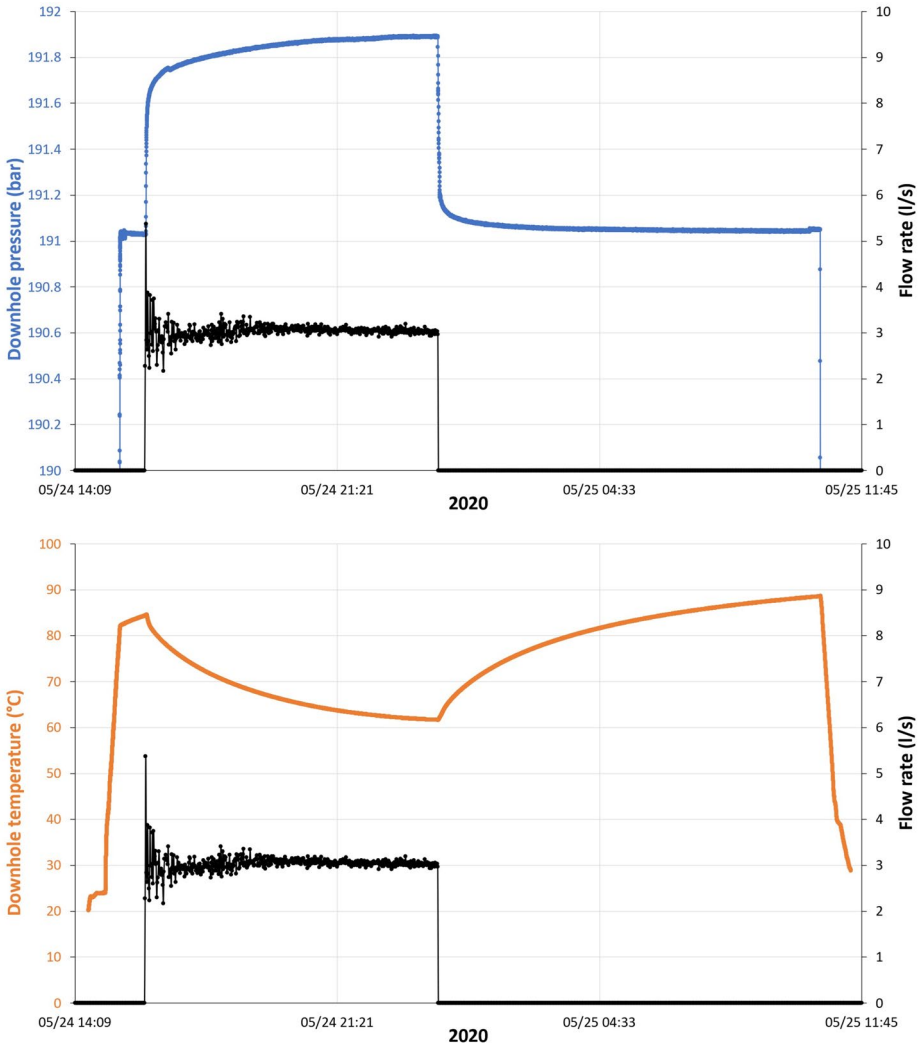


Fig. 14 Downhole pressure (top) and temperature (bottom) recorded at a depth of 1950 m as well as injection rate during the third injection test

Table 11 Components of gel used in hydraulic fracturing

Material	Function	Value
Nalco 73,500	Bactericide	40 l
Caustic Soda	pH control	10 kg
Incorr	Corrosion inhibitor	40 l
VISCO XC84	Viscosity enhancer	50 kg
Policell SL	Drying control	150 kg
Intaflow	Bridge builder	200 kg

2nd stimulation experiment: acid treatment and fifth injection test

After the failed fourth injection test, an acid wash was conducted for two reasons. First, it served as a method to remove the previously injected slurry in the well, since

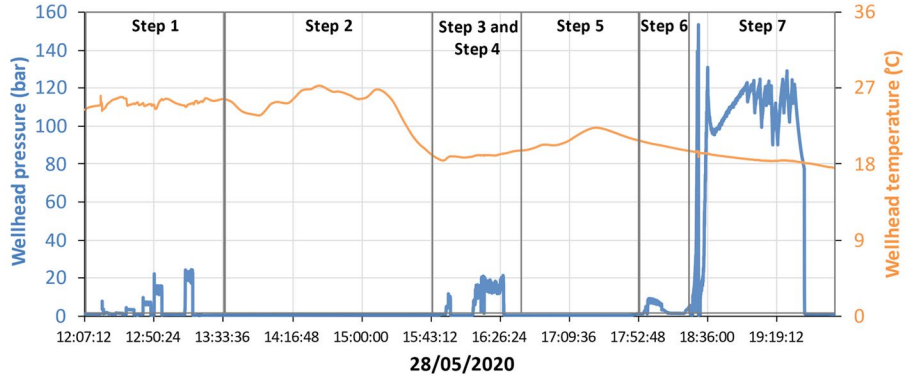


Fig. 15 Wellhead pressure and temperature during hydraulic fracturing with gel and proppant. The steps and the evolution of the flow rate is described in the text

the effect of hydraulic fracturing on well parameters could not be evaluated. Second, the experiment could be used to test the efficiency of enhancing injectivity of the well by the dissolution of calcite precipitation as part of the stimulation program. Therefore, chemical stimulation using 15% HCl was performed. The treatment was conducted on 03.06.2020 in the following way:

1. 11:20–11:55: Injection of 15% HCL at 3.3 l/s flow rate;
2. 11:55–12:05: Injection of 1 m^3 water;
3. 12:15–12:45: Injection of 7 m^3 water for settling. No pressure change at well-head;
4. 12:45–14:45: Acid attack in the formation.

The efficiency of the chemical stimulation was evaluated in the fifth injection test (Test #8, Fig. 16). In this experiment, water is injected at several steps with average flow rates of 1.2, 3.3 and 4.2 l/s. The test results reveal a permeability of 3.96 10^{-12} m^2 (3960 mD), transmissibility of 4.35 10^{-11} m^3, a skin of 20 and an injectivity index of 0.4 l/(s bar). The very large skin factor reveals poor near-wellbore flow performance.

Pump lift and sixth injection test

Since the latest tests demonstrated a significant decrease in injectivity index and large skin factor, pump lift was performed to clean the wellbore from potential stimulation fluid residuals. The production flow rates varied between 16.7 and 20 l/s at an average wellhead pressure of 18 bar between 09 and 12.06.2020 resulting in a total produced fluid of 888 m^3.

The evaluation of the subsequent sixth injection test performed with 5, 8.5, 11 l/s average flow rates (Fig. 17) shows that the permeability is 3.12 10^{-12} m^2 (3120 mD), the transmissibility is 3.44 10^{-11} m^3, the injectivity index is 5.6 l/(s bar). The well shows a strong negative skin of -6.7.

3rd stimulation experiment: skin frac treatment and eighth injection test

In 2021, the skin frac treatment was conducted. The test design and material needs were determined based on the tests described above, previous skin frac campaigns performed in commercial offset oil and gas wells as well as using the FracPro commercial hydraulic

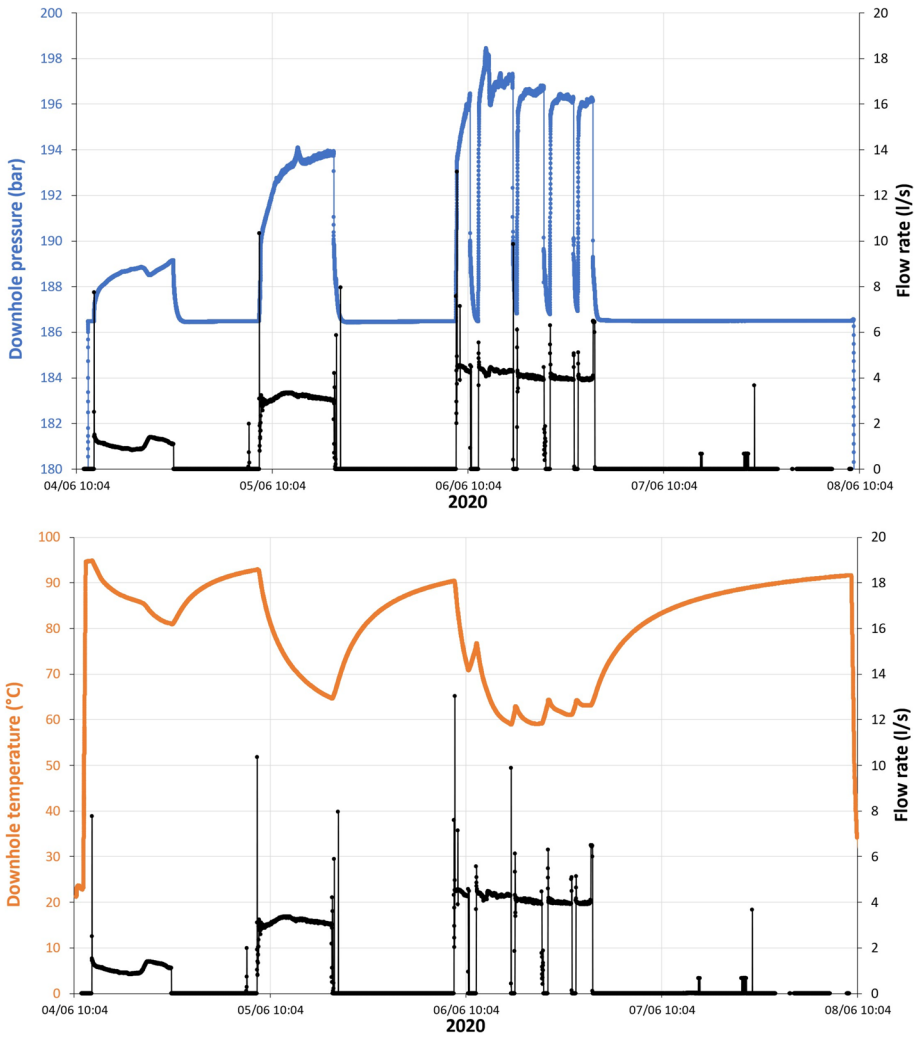


Fig. 16 Downhole pressure (top) and temperature (bottom) recorded at a depth of 1950 m as well as injection rate during fifth injection test

Table 12 Input formation parameters of the FracPro hydraulic fracturing simulator

Parameter	Value
Permeability (m^2)	$5\ 10^{-13}$
Porosity (%)	30
Reservoir pressure (Pa)	$2\ 10^{7}$
Pore fluid viscosity (Pa s)	$1\ 10^{-3}$
Fracture pressure gradient (Pa/km)	$1.1\ 10^{7}$
Young's modulus (Pa)	$3.5\ 10^{9}$
Poisson's ratio (-)	0.3
Fracture toughness (Pa $m^{1/2}$)	$3.8\ 10^{6}$
Total compressibility (1/Pa)	$9.71\ 10^{-10}$

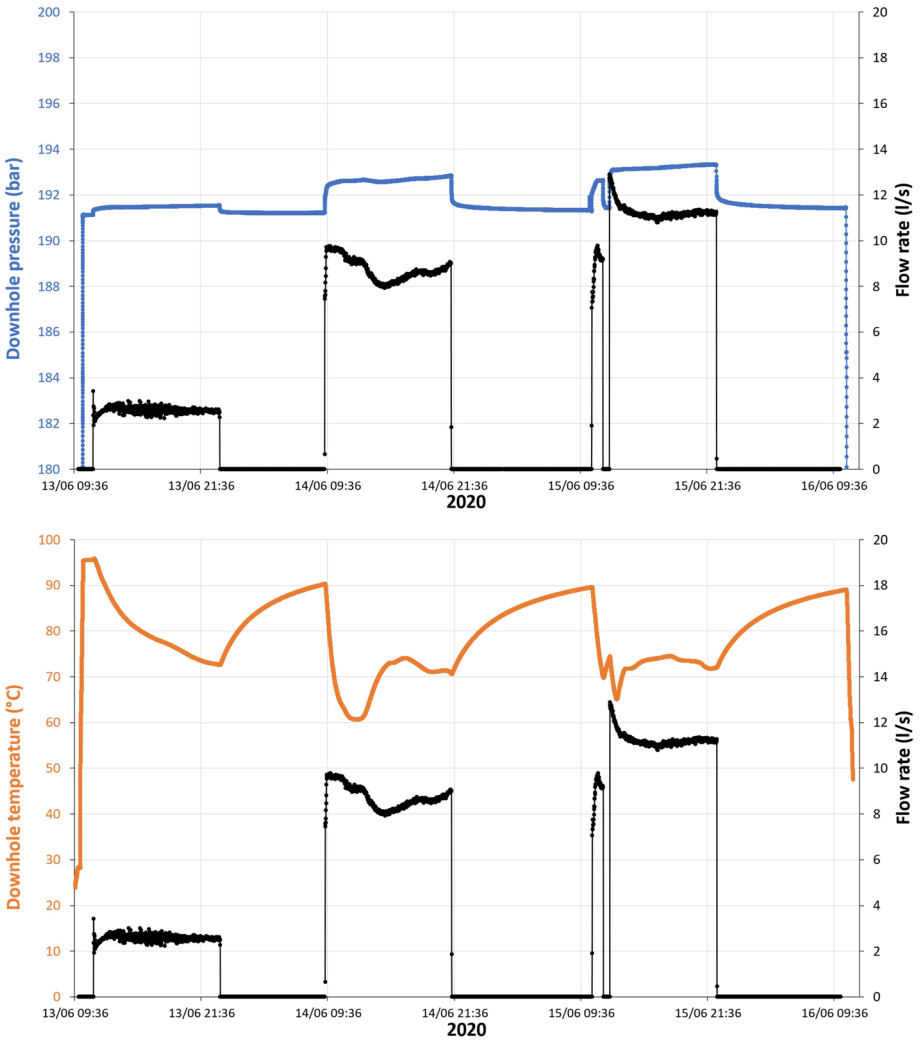


Fig. 17 Downhole pressure (top) and temperature (bottom) recorded at a depth of 1950 m as well as injection rate during the sixth injection test

fracturing simulator. The well structure provided in Table 6 is used in the simulations. Based on that, the available borehole flush volume to 2032 m depth is 4.548 m^3. The hydraulic and mechanical parameters of the sandstone formation used in the model are summarized in Table 12 based on Table 4 and Farkas et al. (2019).

The fluid recipe of the fracturing fluid was designed by Newpark Fluid Systems. The stimulation fluid to be pumped for 6 h was aimed at having a minimal viscosity above 500 mPa s (5 10^{-1} Pa s) at the formation temperature of 105 °C that can allow for efficient proppant transport and placement. Then the fluid viscosity completely breaks (strongly reduces) between 6 and 24 h after injection. Regarding proppant selection, based on the sand test results in Figs. 5 and 6, the suggested mesh size is 20/40. However, due to economic reasons, it was decided to use a smaller size of 30/50. Since both induced fracture surface properties and closure pressure are expected to have stronger effect on fracture conductivity compared to proppant particle size (Tian et al. 2024), thus, this economic decision should not significantly influence the treatment.

Table 13 Simulated schedule for the skin frac experiment

Stage no	Stage Type	Elapsed Time (min:sec)	Fluid Type	Clean Volume (m^3)	Proppant concentration (kg/m^3)	Stage Proppant (tons)	Slurry Rate (l/s)	Proppant Type	Purpose
Wellbore fluid			DynaFrac HT 35	4.548					Borehole volume
1	Main frac pad	3:59	DynaFrac HT 35	4.548	0	0.0	16.7		Induce hydrofrac that can sustain proppants
2	Main frac slurry	6:02	DynaFrac HT 35	1.452	60	0.1	16.7	Sintered bauxite 30/50	Filling proppant into the propagating hydraulic fracture. Proppant concentrations are increased sequentially
3	Main frac slurry	7:04	DynaFrac HT 35	1.000	120	0.1	16.7		
4	Main frac slurry	8:06	DynaFrac HT 35	1.000	160	0.2	16.7		
5	Main frac slurry	9:09	DynaFrac HT 35	1.000	180	0.2	16.7		
6	Main frac slurry	10:14	DynaFrac HT 35	1.000	240	0.2	16.7		
7	Main frac slurry	11:20	DynaFrac HT 35	1.000	360	0.4	16.7		
8	Main frac slurry	12:27	DynaFrac HT 35	1.000	400	0.4	16.7		
9	Main frac slurry	13:37	DynaFrac HT 35	1.000	600	0.6	16.7		
10	Main frac slurry	14:47	DynaFrac HT 35	1.000	600	0.6	16.7		
11	Main frac slurry	15:57	DynaFrac HT 35	1.000	600	0.6	16.7		
12	Main frac slurry	17:08	DynaFrac HT 35	1.000	600	0.6	16.7		
13	Main frac flush	21:40	Slickwater	4.548	0	0.0	16.7		Flushing borehole

According to the simulator, the specific fluid type is similar to DynaFrac HT 35. Under these conditions a propped, radial hydraulic fracture with the highest dimensionless fracture conductivity (F_C) of 0.43 with a maximum half-length of 6 m and average width of 1.73 cm over the entire perforation interval II can be achieved using sintered bauxite proppant with 30/50 mesh size.

Table 13 summarizes the design treatment and Fig. 18 shows the simulated pressure evolution. According to the latter, the formation breakdown pressure is at approx. 160 bar well-head pressure and it occurs within the first minute. The creation of a hydraulic fracture lasts for approx. 4 min and the arresting of its growth by tip screen out (TSO) as well as fracture inflation and gradual proppant packing should last until 17 elapsed minutes. Between 17 and 22 elapsed minutes, borehole flush using slickwater is reflected in decreasing wellbore friction (red curve in

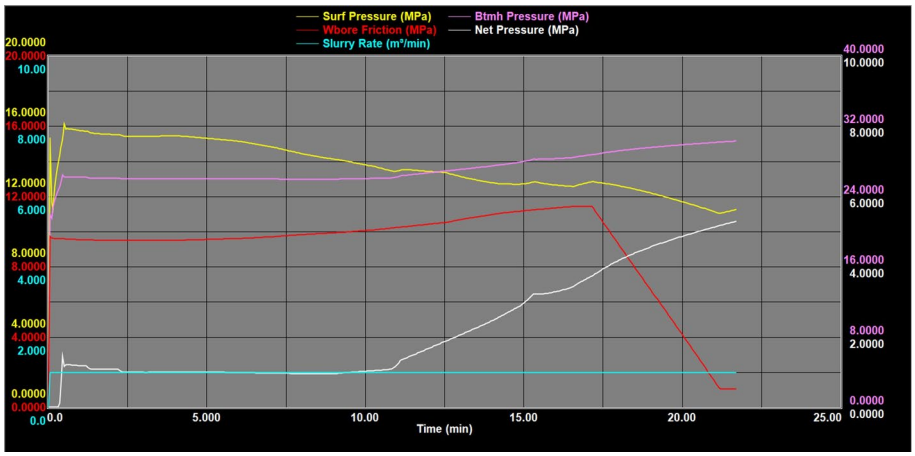


Fig. 18 Simulation results of suggested treatment for skin frac experiment in well SZT-VIII

Fig. 18). The suggested injection rate throughout the treatment is 16.7 l/s. The calculated material needs are 16 m^3 gel and 4 tons of sintered bauxite proppant with mesh size of 30/50.

Based on the simulation results, a pump with max 350 bar pressure, 2 batch mixers with 10 m^3 volume, 2 big bags (4 tons) of Saint–Gobain sintered bauxite proppant with 30/50 mesh size were used for the experiment. The field experimental setup is illustrated in Fig. 19.

Seventh injection test

The first phase of the operation with water injection (Test #11a) aimed at testing the hydraulic behaviour of the system with flow rates of 4.2, 16.7 and 20 l/s (Fig. 20). This phase shows that the maximum well-head pressure (WHP) of 110 bar is larger compared to the pressure level for non-linear flow behavior determined in the 1st step rate test (Test #3), but there is no indication for leak-off or reaching the formation breakdown pressure. This observation agrees with the FracPro simulation of the main treatment using slurry (gel and proppant), where fracturing pressure is reached at $WHP = 160$ bar.

Second step-rate test

The second phase, a step-rate (Test #11b) test using water aimed at identifying possible non-linearities in flow behavior (Fig. 21). According to Fig. 22, both Test #11a and #11b show higher injectivity compared to 1st step-rate test (Test #3).

Skin frac test

The third, main treatment phase (Test #11c) served as transmissibility and injectivity enhancement period consisting of hydraulic fracturing (skin frac) and gel displacement periods (Fig. 23). The injected proppant mass was not recorded, but it was pumped at a rate according to design schedule in Table 13. During the low injection rate step of 6.7 l/s, injection was stopped for a minute due to pump outage. After the pump outage, the injection was continued at constant rate, where pressure increased



Fig. 19 View of the site during the skin frac operation

despite increasing proppant concentration. At about 10 l/s injection rate level, the pressure increases to 170 bar well-head pressure and at about 13.3 l/s rate, the peak pressure reaches 200 bar *WHP*. Both pressure levels are above the calculated fracturing pressure of 160 bar. This pressure evolution is in contrast to a similar experiment reported by Zimmermann and Reinicke (2010), where the pressure decreased in this phase. The unexpected behavior could be explained either by blocking effects of the slurry in the well during pump outage. After the skin frac experiment, gel displacement (borehole flush) was conducted. Based on well test analysis of that phase, the calculated permeability is 1.07 10^{-11} m^2 (10,700 mD), the transmissibility is 1.18 10^{-10} m^3, and skin is − 2.61.

The subsequent eighth injection test (Test #12), few days after the skin frac operation shows a significant change in the well test parameters: permeability is 3.36 10^{-12} m^2 (3360 mD), the transmissibility is 3.7 10^{-11} m^3, skin is 6 and the injectivity index is 3.6 (Fig. 24 and Table 9).

Discussion

Well and reservoir behaviour

The analysis of permeability and transmissibility, skin and injectivity index can be discussed as follows. Test #1, where all perforation intervals are tested hydraulically,

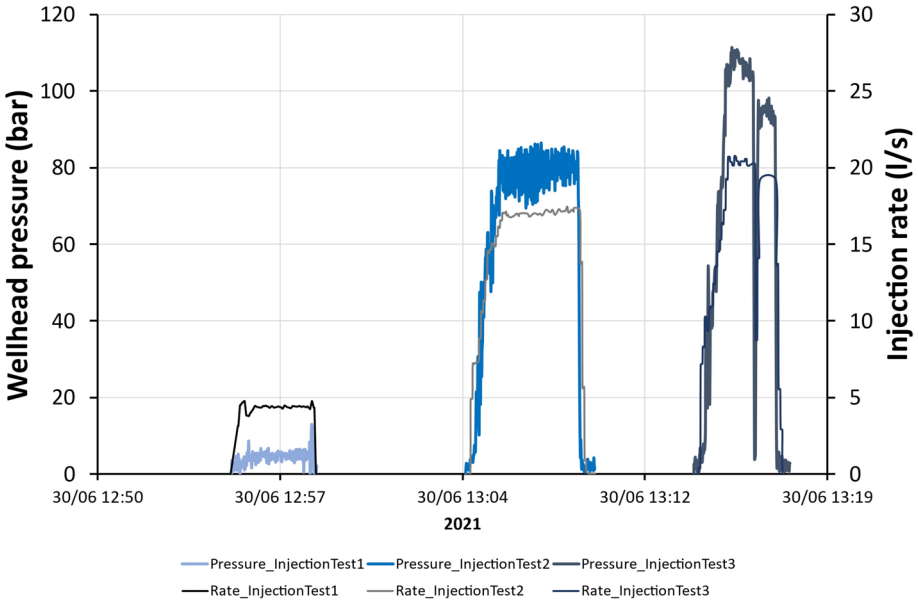


Fig. 20 Pressure and injection rate records during initial injection tests before the skin frac treatment

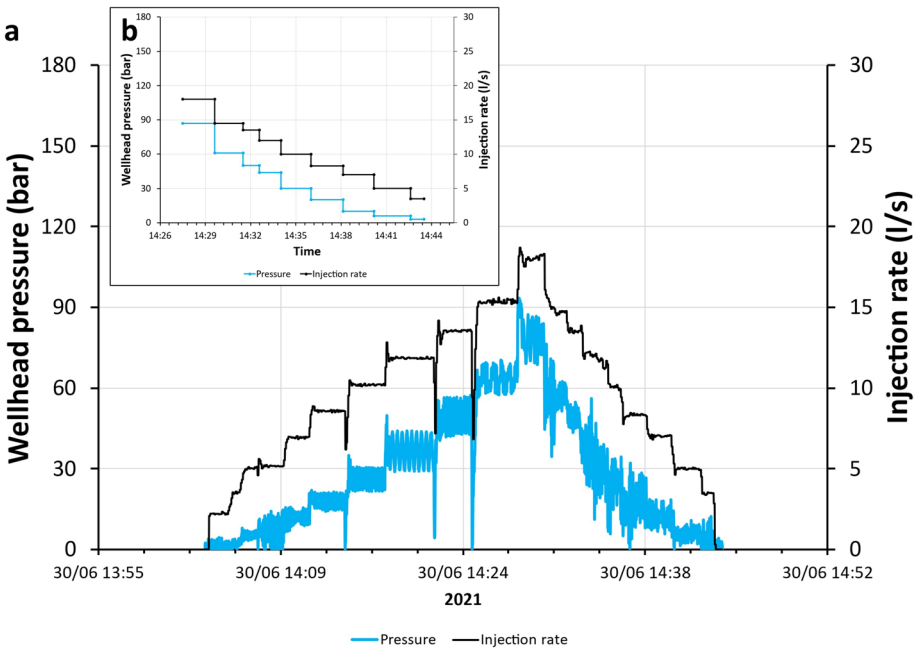


Fig. 21 Pressure and injection rate records during step-rate test before the skin frac treatment (**a**). Smoother pressure representation for the step down phase is provided in figure inlet (**b**)

exhibits a high skin factor larger than 5, which indicates formation damage in the well. Since the well has been only used for production over decades, thus, it can be assumed that the formation damage may be associated with sand and fine migration, which is also shown by debris in the well prior to operation. The intervention, i.e., the isolation of the perforation interval with the highest inflow rate results in more favorable, negative skin factor of − 5.16 (Test #2). This is an interesting result, since it

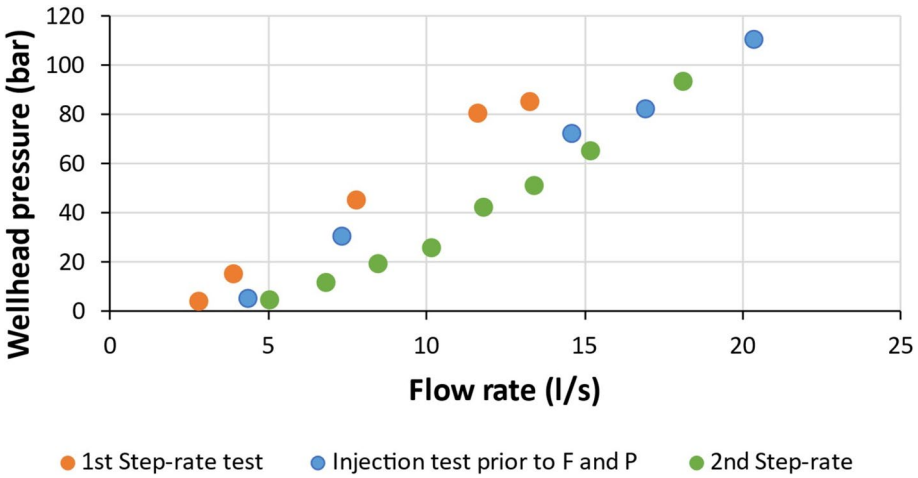


Fig. 22 Comparison of injectivity between 1st step-rate test (Test #3), injection (Test #11a) and 2nd step-rate test (Test #11b) prior to skin frac experiment (Test #11c)

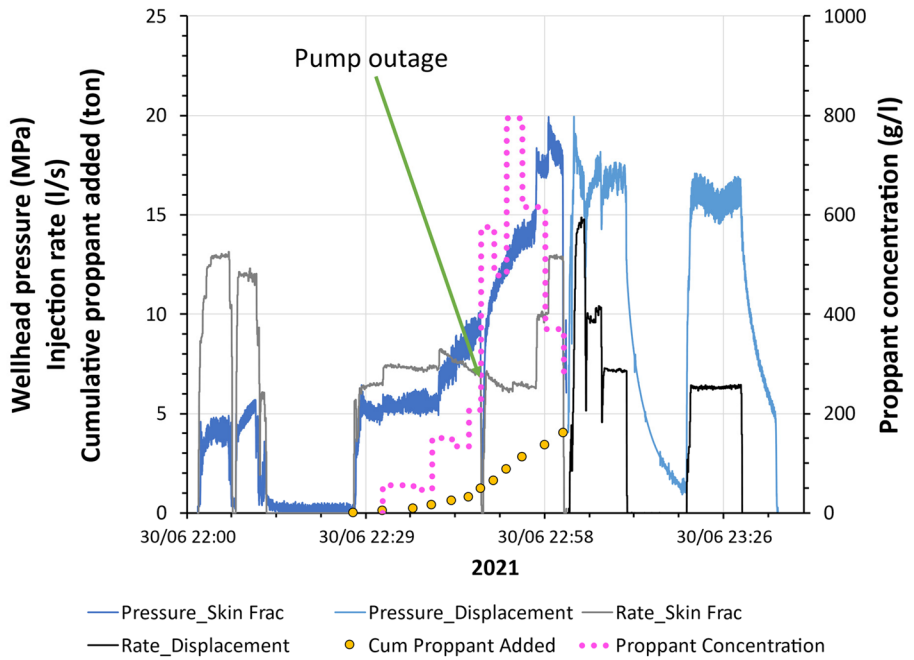


Fig. 23 Pressure, injection rate, cumulative proppant and proppant concentration records during hydraulic fracturing and gel displacement of the skin frac treatment. To enhance visibility, we use MPa unit for pressure here

indicates a significant fracture, although neither geophysical logging nor the injection test (Test #2) suggests any hint towards fracture induction or flow into reopened fracture. However, since cold water was injected into the interval, the possibility of thermal or compaction-induced fracturing should be investigated in the future, e.g., using thermal–hydro–mechanical coupled modeling. Another interesting observation is that the injectivity index of the best performing interval is about 10% higher than that

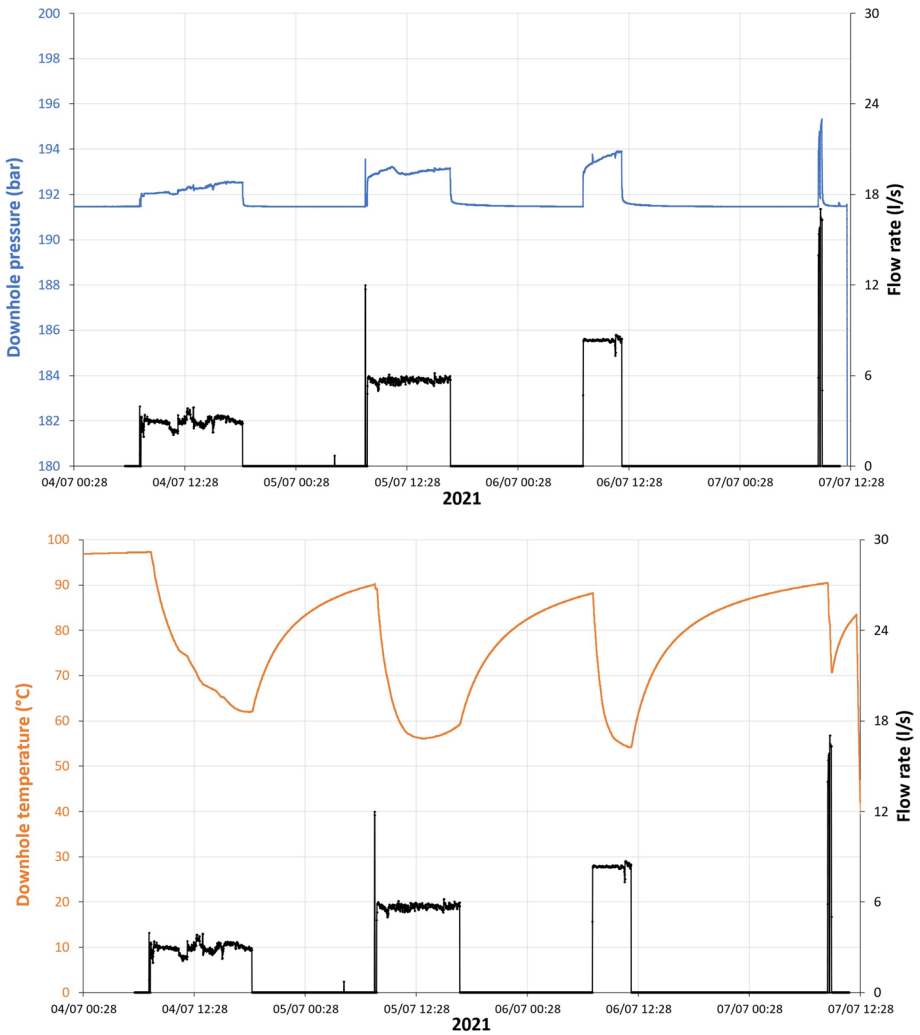


Fig. 24 Downhole pressure recorded at a depth of 1950 m and injection rate during the eighth injection test

considered for all intervals. This implies that this interval is worth for stimulation to enhance injectivity despite the skin of -5.

After diagnostic step-rate test 1 in the isolated interval (Test #3), the subsequent injection test (Test #4) reveals that skin factor becomes significantly larger, i.e., 8.9 and injectivity decreases by 10% compared to prior-to-test conditions. The high skin factor implies considerable formation damage, which occurs after 1-h-long step-rate injection test. The rapid decrease in well injectivity in loose sedimentary rock is also reported by Zettlitzer et al. (2010), where CO_2 was injected in loose sandstone of Stuttgart Formation at the former pilot CO_2 storage site in Ketzin, Germany.

Unfortunately, the effect of the first and second remediation techniques, hydraulic fracturing (Test #5) and acid treatment (Test #7) on the wellbore behavior can be only evaluated jointly, since the injection test after the former experiment (Test #6) was unsuccessful. Thus, it is not fully understood why all studied well parameters are the poorest after these experiments (Test #8), i.e., skin of 20 and injectivity index of 0.4 l/(s bar). The lack of injectivity increase or skin improvement due to acid treatment in

contrast to successful test at the same formation under similar conditions in Mezőberény reported by Brehme et al. (2024) may be linked to the absence of well clean-up after the hydraulic fracturing or to the lower total dissolved solids (salinity) and bicarbonate content of the brine in the Szentes area. The lower salinity and bicarbonate content in well SZT-VIII compared to the referred study implies lower tendency for scaling: 2310 vs 6705 mg/l of total dissolved solids as well as 1629 mg/l vs 4470 mg/l of HCO_3, respectively. However, a geochemical model may provide quantitative information regarding the formation of well clogging due to precipitation of carbonate mineral.

Interestingly, pump lift operation (Test #9), which was not part of the original stimulation program, managed to improve wellbore conditions (Test #10). Skin and injectivity index are not only restored compared to previous state determined in Test #8, but both exhibit the best values achieved in the stimulation program compared to Test #2, i.e., -6.67 vs -5.16 and 5.6 l/ (s bar) vs 4.1 l/ (s bar), respectively. Thus, pump lift proves to be an efficient operation for well remediation, as also shown by Zhang et al. (2022) in a geothermal well and Zettlitzer et al. (2010) in a well-used for injecting CO_2 in poorly consolidated sandstone rock.

Since no further skin and injectivity enhancement can be expected for the studied interval II, skin frac was performed on interval I and II (Test #11), where interval I previously showed poor inflow (Table 10). The results of the skin frac operation show temporary successful treatment. Permeability is increased by one order of magnitude compared to Test #1, and a skin of − 2.6 agrees with the expected value for such treatment by Nitters et al. (2016). Consequently, performance in both near- and far-well area are improved. However, the well test analysis of the subsequent injection test (Test #12) reveals permeability, skin and injectivity values almost identical to Test #1. This suggests that the induced hydraulic fracture could be propped only temporarily, and it must have closed, probably due to pump outage during operation or not sufficiently large proppant mesh size.

Implications for field operation

The results also allow making implications for field operation while considering underlying clogging mechanisms in the well. Out of the four stimulation treatments, hydraulic fracturing and acid treatment did not deliver any improvement to the well, neither in the near nor in the far-wellbore area. This suggests that reservoir transmissibility is not linked to any potential injection-related issue and chemical clogging is probably not a dominant clogging process. On the other hand, skin frac experiment temporarily reached its both near and far-wellbore goals. Furthermore, the unplanned pump lift delivered significant improvement in near-wellbore area compared to base case. These results imply that injectivity in the well is controlled by potential formation damage induced by mechanical clogging due to mobilization of fine particles of the sandstone rock formation.

The results agree with those reported by You et al. (2019), Zettlitzer et al. (2010) and Zhang et al. (2022) who conducted an experimental and numerical study on formation blockage risk analysis of thermal water reinjection in a geothermal well screened at weakly cemented sandstones. Similar to the well in the present study, that well is reported to exhibit high productivity and permeability, but low injectivity due to

mobilization and deposition of fine (sand and clay) particles. The authors conclude that pump lift is an effective measure to remove the well blockage on a regular basis to maintain the desired injectivity of the well for a longer time.

Learnings, limitations and future work

Table 14 compares the applied stimulation methods with respect to observed effects. Based on the results, although the effect of hydraulic fracturing cannot be evaluated, it is likely not an optimal treatment due to large reservoir permeability. As for acid treatment, additional hydrogeochemical modelling may be conducted to estimate the amount of mineral phases that may precipitate in sodium carbonate formation water leading to formation damage due to long-term reinjection. Pump lift proves to be an efficient measure to restore skin and injectivity to produce deposited solid particles due to formation damage. According to Zhang et al. (2022), this may be conducted once injectivity drops by half or the reinjection pressure doubles. Furthermore, injection rate can be also temporarily increased to mitigate clogging. However, in the long term, this approach may deteriorate reservoir mechanical properties. Thus, skin frac may provide a stable intervention. Its short-term enhancement of wellbore skin is demonstrated, albeit further investigation with improved experimental design is required to prove its long-term feasibility.

Some limitations must be considered in the interpretation of the results. It remains open why the other, not tested perforated intervals of the well exhibit much lower injectivity based on flow meter and temperature logs. It is, therefore, suggested to separately conduct separate injection tests in these intervals to identify possible mechanisms. An optimization approach could also look into occasional diverter drops that could reroute the fluid flow for injectivity and distribution along the injection pay, or bioballs. Furthermore, it is suggested to conduct skin frac experiment with larger mesh size to achieve propped hydraulic fracture permanently as well as a fluid recipe that allows fluid losing viscosity much faster.

It must be also pointed out that the framework proposed by Markó et al. (2021), which is also applied in the current study to investigate injection-related phenomena in geothermal wells does not consider the possible effect of reservoir subsidence due to reservoir overexploitation. The Szentes geothermal field has been producing since the 1960s without reinjection, which represents a substantial timeframe for pressure

Table 14 Comparison of the applied stimulation techniques

Stimulation method	Observed effect	Comment
Hydraulic fracturing	Further investigation is needed	Likely not necessary treatment due to large reservoir permeability
Acid treatment	No clear conclusion, further investigation is needed	Additional hydrogeochemical modelling may quantify the likeliness of formation damage
Pump lift	Enhanced near-wellbore effects: decrease in skin and increase in injectivity	Best skin and injectivity values observed after pump lift. Recommended procedure for field operators
Skin frac	Temporary performance enhancement both in near- and far-well area	Further investigation with optimal experimental design is needed

depletion and subsequent compaction to occur. This long-term deformation could significantly impact the mechanical properties and flow behavior of the poorly consolidated sandstone rock. Subsidence affects the stress field around the wells, which may result in fracturing. Furthermore, such fractures may not be optimally oriented for fluid flow. Thus, future work should aim at better understanding the complex interaction between production history, changes in geomechanical rock properties, and injectivity performance in planning long-term reinjection tests.

Conclusions

The hot geothermal reservoir in the Szentes geothermal field in Hungary is characterized by high reservoir permeability, but with injectivity insufficient for long-term reinjection of thermal water into the unconsolidated Upper Pannonian sandstone formation. To ensure stable injectivity, several stimulation techniques were applied, including hydraulic fracturing, acid injection, skin frac test. In addition, pump lift was also conducted in the well.

Based on the experimental results, we draw the following conclusions.

1. The field test results suggest that particle migration and resulting mechanical clogging in near-wellbore area is the dominant process responsible for reduced injectivity.
2. Pump lift delivered injectivity enhancement. The propped fracture treatments resulted in poor performance for long-term injection.
3. This is the first study that reports on a skin frac completion in a geothermal well. The technique was capable of temporary permeability enhancement, but further field demonstration with optimized design is required to prove its long-term feasibility.
4. Future work will consider coupled modelling of clogging processes during long-term reinjection of thermal water in a newly drilled well in the same reservoir and laboratory experiments that aim to reproduce these processes. This includes understanding particle mobilization and deposition as well as the effect of reservoir compaction due to overexploitation.

Acknowledgements
We would like to express our sincere gratitude to Mecsekérc Ltd for their support in data preparation and interpretation. We would also like to thank the Reviewers for taking the time and effort necessary to review the manuscript. We sincerely appreciate all valuable comments and suggestions, which helped us to improve the quality of the manuscript.

Author contributions
MPF and GM measured and analyzed the data, prepared the figures, and wrote the manuscript. GM, HH, GZ and FF helped in designing the study and contributed to the interpretation and discussion of the results. All the authors read and approved the final manuscript.

Funding
Open Access funding enabled and organized by Projekt DEAL. This research was funded by the Hungarian National Research, Development, and Innovation Office (NKFIH) (grant number GINOP-2.2.1–15-2017–00102). This work was also supported by the Helmholtz Association's Initiative and Networking Fund for the Helmholtz Young Investigator Group ARES (contract number VH-NG-1516) and by the European Regional Development Fund for the Interreg Central Europe project TRANSGEO (contract number CE0100071).

Availability of data and materials
All data generated or analyzed during this study are included in this paper.

Declarations

Ethics approval and consent to participate
Not applicable.

Competing interests
The authors declare no competing interests.

Received: 23 September 2024 Accepted: 10 April 2025
Published online: 30 April 2025

References

Almási I. Petroleum hydrogeology of the great Hungarian plain, Eastern Pannonian Basin, Hungary. PhD Thesis, University of Alberta. 2001.
Bálint A, Szanyi J. A half century of reservoir property changes in the Szentes geothermal field, Hungary. Central Eur Geol. 2015;58(1–2):28–49.
Békési E, Fokker PA, Candela T, Szanyi J, van Wees JD. Ground motions induced by pore pressure changes at the Szentes geothermal area, SE Hungary. Geothermal Energy. 2022;10:3.
Blöcher G, Peters E, Reinsch T, Petrauskas S, Valickas R, van den Berg S. D3.2 Report on radial jet-drilling (RJD) stimulation technology. Deliverable for the European Horizon Europe Project SURE. 2016.
Brehme M, Markó Á, Osvald M, Zimmermann G, Weinzierl W, Aldaz S, Thiem S, Huenges E. Demonstration of a successful soft chemical stimulation in a geothermal sandstone reservoir in Mezőberény (Hungary). Geothermics. 2024;120: 102980.
Budai S, Willems CJL, Colombera L, Westaway R. Influence of sedimentary architecture on static connectivity and geothermal doublet performance (Mezőberény, SE Hungary). Mar Pet Geol. 2024;164: 106820.
Civan F. Formation damage fundamentals—modeling, assessment, and mitigation. Gulf Professional Publishing. 2007.
Cleary M P. Critical Issues in Hydraulic Fracturing of High-Permeability Reservoirs. Paper presented at the European Production Operations Conference and Exhibition, Aberdeen, United Kingdom, March 1994. 1994; Paper Number: SPE-27618-MS.
Croese E, Doddema S, Veeger F. Microbiology in Geothermal Operations. Paper presented at the CORROSION 2019 conference, Nashville, Tennessee, USA, March 2019. 2019; Paper Number: NACE-2019–12818.
Economides MJ, Nolte KG. Reservoir Stimulation. Wiley. 2020.
EGEC (European Geothermal Energy Council) Geothermal market report 2023. In: Dumas P, Kumar S, Martini E, Cittadini G, Mikovics A (eds). Brussels, 2024.
Farkas MP, Yoon JS, Zang A, Zimmermann G, Stephansson O, Lemon M, Dankó G. Effect of foliation and fluid viscosity on hydraulic fracturing tests in mica schists investigated using distinct element modeling and field data. Rock Mech Rock Eng. 2019;52:555–74.
Geissler N, Garsche F, di Mare F, Bracke R. Overview and comprehensive performance description of a new micro turbine drilling—MTD technology for drilling laterals into hard reservoir rock. Int J Rock Mech Min Sci. 2023;161: 105253.
Gelencsér K, Kovács L, Gál V, Zipf Mázik K, Horváth T, Kiss M, Farkas M, Biber Z, Szujó G, Rátkai O. Rock mechanical characterization of natural and artificial rock samples prepared in the framework of GINOP project. Paper presented at the Final Conference of the GINOP project, Pécs, Hungary, October, 2022.
Hofmann H, Zimmermann G, Farkas M, Huenges E, Zang A, Leonhardt M, Kwiatek G, Martinez-Garzon P, Bohnhoff M, Min KB, Fokker PA, Westaway R, Bethmann F, Meier P, Yoon KS, Choi JW, Lee TJ, Kim KY. First field application of cyclic soft stimulation at the Pohang Enhanced Geothermal System site in Korea. Geophys J Int. 2019;217(2):926–49.
Horne RN. Modern well test analysis: a computer-aided approach. 2nd ed. Palo Alto: Petroway Inc; 1995.
Horváth F, Musitz B, Balázs A, Végh A, Uhrin A, Nádor A, Koroknai B, Pap N, Tóth T, Wórum G. Evolution of the Pannonian basin and its geothermal resources. Geothermics. 2015;53:328–52.
Koroncz P, Vizhányó Z, Farkas MP, Kuncz M, Ács P, Kocsis G, Mucsi P, Szász Fedorné A, Fedor F, Kovács J. Experimental Rock Characterisation of Upper Pannonian sandstones from Szentes geothermal field, Hungary. Energies. 2022; 15:(23),9136.
Lee J. Well testing. SPE textbook series, vol. 1, pp. 159, Society of Petroleum Engineers. 1982.
Lenkey L, Mihályka J, Paróczi P. Review of geothermal conditions of Hungary. Földtani Közlöny. 2021;151(1):65–78.
Luo W, Kottsova A, Vardon PJ, Dieudonné AC, Brehme M. Mechanisms causing injectivity decline and enhancement in geothermal projects. Renew Sustain Energy Rev. 2023;185: 113623.
Mádl-Szőnyi J, Markó Á, Tóthi T. Nem lehet mindenhol mindent, de mindenhol lehet valamit – A geotermikus energia hasznosításának lehetőségei a hazai ellátás diverzifikálása érdekében (Not everything anywhere, but something everywhere – geothermal to diversify the domestic energy supply). Sci Securitas. 2024;4(3):153–68.
Markó Á, Mádl-Szőnyi J, Brehme M. Injection related issues of a doublet system in a sandstone aquifer—a generalized concept to understand and avoid problem sources in geothermal systems. Geothermics. 2021;97: 102234.
Markó Á, Brehme M, Pedretti D, Zimmermann G, Huenges E. Controls of low injectivity caused by interaction of reservoir and clogging processes in a sedimentary geothermal aquifer (Mezőberény, Hungary). Geotherm Energy. 2024;12:40.
Martyushev DA, Ponomareva IN, Chernykh VI, Davoodi S, Kazemzadeh Y, Ma T. Impacts of interactions with low-mineralized water on permeability and pore behavior of carbonate reservoirs. Energy Geosci. 2024;5(4): 100340.
Morales RH, Profinet J, Piedras J, Gadiyar B, Harris S. Optimization of Frac/pack completions based on field experience. Paper presented at the SPE Annual Technical Conference and Exhibition, Denver, Colorado, USA, October 2003. 2003; Paper Number: SPE-84263-MS.
Nitters G, Pittens B, Buik N. Well stimulation techniques for geothermal projects in sedimentary basins. Technical Report prepared by IF Technology, Arnhem, the Netherlands, 2016.

Njeru RM, Halisch M, Szanyi J. Micro-scale investigation of the pore network of sandstone in the Pannonian Basin to improve geothermal energy development. Geothermics. 2024a;122: 103071.
Njeru RM, Sofyan A, Halisch M, Kóbor B, Szanyi J. Optimizing micro-CT resolution for geothermal reservoir characterization in the Pannonian basin. Energies. 2024b;17:3081.
Ochi J, Vernoux JF. Permeability decrease in sandstone reservoirs by fluid injection: hydrodynamic and chemical effects. J Hydrol. 1998;208(3–4):237–48.
Park S, Kim KI, Xie L, Yoo H, Min KB, Kim M, Yoon B, Kim KY, Zimmermann G, Guinot F, Meier P. Observations and analyses of the first two hydraulic stimulations in the Pohang geothermal development site, South Korea. Geotherm. 2020;88: 101905.
Portier S, André L, Vuataz FD. Review on chemical stimulation techniques in oil industry and applications to geothermal systems. Technical Report for ENhanced Geothermal Innovative Network for Europe (ENGINE) project, Work Package 4. 2007.
Roodhart LP, Fokker PA, Davies DR, Shlyapobersky J, Wong GK. Frac-and-pack stimulation: application, design, and field experience. J Petrol Technol. 1994;46:230–8.
Rosenbrand E, Haugwitz C, Jacobsen PSM, Kjøller C, Fabricius IL. The effect of hot water injection on sandstone permeability. Geothermics. 2014;50:155–66.
Seibt P, Kellner T. Practical experience in the reinjection of cooled thermal waters back into sandstone reservoirs. Geothermics. 2003;32:733–41.
Szanyi J, Kovács B. Utilization of geothermal systems in south-east Hungary. Geothermics. 2010;39(4):357–64.
Szanyi J, Nádor A, Madarász T. A Geotermikus Energia Kutatása És Hasznosítása Magyarországon Az Elmúlt 150 Év Tükrében (geothermal energy exploration and utilization in Hungary in the past 150 Years). Földtani Közlöny. 2021;151(1):79–102.
Tian F, Jia Y, Yang L, Liu X, Guo X, Martyushev DA. Experimental study on factors affecting fracture conductivity. Processes. 2024;12(7):1465.
Ungemach P. Reinjection of cooled geothermal brines into sandstone reservoirs. Geothermics. 2003;32:743–61.
Varga A, Bozsó G, Garaguly I, Raucsik B, Bencsik A, Kóbor B. Cements, waters, and scales: an integrated study of the Szeged geothermal systems (se Hungary) to characterize natural environmental conditions of the thermal aquifer. Geofluids. 2019;2019:4863814.
Willems C, Cheng C, Watson S, Minto J, Williams A, Walls D, Milsch H, Burnside N, Westaway R. Permeability and mineralogy of the Újfalu formation, Hungary, from production tests and experimental rock characterization: implications for geothermal heat projects. Energies. 2021;14:4332.
You Z, Badalyan A, Yang Y, Bedrikovetsky P, Hand M. Fines migration in geothermal reservoirs: laboratory and mathematical modelling. Geothermics. 2019;77:344–67.
Zettlitzer M, Moeller F, Morozova D, Lokay P, Würdemann H. Re-establishment of the proper injectivity of the CO_2-injection well Ktzi 201 in Ketzin, Germany. Int J Greenhouse Gas Control. 2010;4:952–9.
Zhang L, Geng S, Yang L, Wen R, He C, Zhao Z, Qin G. Formation blockage risk analysis of geothermal water reinjection: Rock property analysis, pumping and reinjection tests, and long-term reinjection prediction. Geosci Front. 2022;13: 101299.
Zhao Y, Wang Y, Wen S, Zhang L, Cao Z, Zhao Z, Xiong W, Cao C, Tang R, Fan Y, Xie Z, Zhang R, Zhou X, Martyushev D, Zhang T. In-situ experiments of dynamic microscopic reaction for CO_2-brine-carbonate system. Chem Eng J. 2025;506: 160251.
Zimmermann G, Reinicke A. Hydraulic stimulation of a deep sandstone reservoir to develop an enhanced geothermal system: laboratory and field experiments. Geothermics. 2010;39(1):70–7.

Publisher's Note

Springer Nature remains neutral with regard to jurisdictional claims in published maps and institutional affiliations.